




Oxidized phospholipids cause changes in jejunum mucus that induce dysbiosis and systemic inflammation

Pallavi Mukherjee¹, Arnab Chattopadhyay¹, Victor Grijalva¹, Nasrin Dorreh¹, Venu Lagishetty^{2,3} , Jonathan P. Jacobs^{2,3,4} , Bethan L. Clifford⁵, Thomas Vallim^{1,5} , Julia J. Mack¹ , Mohamad Navab¹, Srinivasa T. Reddy^{1,6,*}, and Alan M. Fogelman¹

¹Division of Cardiology, ²The Vatche and Tamar Manoukian Division of Digestive Diseases, and ³UCLA Microbiome Center, Department of Medicine, David Geffen School of Medicine at UCLA, Los Angeles, CA, USA; ⁴The Division of Gastroenterology, Hepatology and Parenteral Nutrition, Veterans Administration Greater Los Angeles Healthcare System Los Angeles, Los Angeles, CA, USA; ⁵Department of Biological Chemistry, and ⁶Department of Molecular and Medical Pharmacology, David Geffen School of Medicine at UCLA, Los Angeles, CA, USA

Abstract We previously reported that adding a concentrate of transgenic tomatoes expressing the apoA-I mimetic peptide 6F (Tg6F) to a Western diet (WD) ameliorated systemic inflammation. To determine the mechanism(s) responsible for these observations, *Ldlr*^{-/-} mice were fed chow, a WD, or WD plus Tg6F. We found that a WD altered the taxonomic composition of bacteria in jejunum mucus. For example, *Akkermansia muciniphila* virtually disappeared, while overall bacteria numbers and lipopolysaccharide (LPS) levels increased. In addition, gut permeability increased, as did the content of reactive oxygen species and oxidized phospholipids in jejunum mucus in WD-fed mice. Moreover, gene expression in the jejunum decreased for multiple peptides and proteins that are secreted into the mucous layer of the jejunum that act to limit bacteria numbers and their interaction with enterocytes including regenerating islet-derived proteins, defensins, mucin 2, surfactant A, and apoA-I. Following WD, gene expression also decreased for *IL36γ*, *IL23*, and *IL22*, cytokines critical for antimicrobial activity. WD decreased expression of both *Atoh1* and *Gfi1*, genes required for the formation of goblet and Paneth cells, and immunohistochemistry revealed decreased numbers of goblet and Paneth cells. Adding Tg6F ameliorated these WD-mediated changes. Adding oxidized phospholipids *ex vivo* to the jejunum from mice fed a chow diet reproduced the changes in gene expression *in vivo* that occurred when the mice were fed WD and were prevented with addition of 6F peptide.  We conclude that Tg6F ameliorates the WD-mediated increase in oxidized phospholipids that cause changes in jejunum mucus, which induce dysbiosis and systemic inflammation.

Interleukins 36 (IL-36), 23 (IL-23), and 22 (IL-22) • Paneth cells • goblet cells • *Akkermansia muciniphila*

The main protein in high density lipoprotein (HDL) is apolipoprotein A-I (apoA-I), which contains 243 amino acids. Peptide mimetics of apoA-I with 10% or less of the number of amino acid residues in apoA-I have been reported by multiple laboratories to bind lipids similar to apoA-I. Most of our work has focused on apoA-I mimetic peptides that are class A amphipathic helical peptides with 18 amino acid residues arranged in a sequence that is not homologous with any portion of the amino acid sequence of apoA-I. However, these mimetic peptides have a tertiary structure that allows them to bind nonoxidized lipids similar to apoA-I. Mimetic peptides with 18 amino acid residues that contained 4–6 phenylalanine residues on the hydrophobic face (named 4F, 5F, and 6F) were found to bind oxidized lipids (particularly oxidized phospholipids) with much higher affinity than apoA-I. Despite their much smaller size, the cost of chemically synthesizing these mimetic peptides is prohibitively high for the treatment of chronic diseases (1). Consequently, our laboratory developed a transgenic tomato that expresses the 6F peptide (1). As a control, a transgenic tomato without the 6F peptide was also generated and named EV (1). The content of the potent tomato antioxidant, lycopene, was slightly higher in wild-type and in the EV control tomatoes compared with the transgenic tomatoes expressing the 6F peptide. However, adding the transgenic tomatoes expressing the 6F peptide to a Western diet (WD) that was fed to *Ldlr*^{-/-} mice inhibited aortic atherosclerosis, but adding the control EV tomatoes did not (1). After feeding WD to which transgenic tomatoes expressing the 6F peptide had been added, intact 6F peptide was found only in the lumen of the small intestine and not in the plasma

Supplementary key words Apolipoprotein A-I (apoA-I) mimetic peptides • atherosclerosis • regenerating islet-derived family members 3 alpha (Reg3a), 3 beta (Reg3b), and 3 gamma (Reg3g) • lipopolysaccharide (LPS) • mucin 2 (Muc2) • surfactant A •

*For correspondence: Srinivasa T. Reddy, sreddy@mednet.ucla.edu.



(1). Despite the absence of 6F peptide in plasma, feeding the transgenic tomatoes expressing the 6F peptide dramatically improved disease processes in animal models in which inflammation plays an important role (1–9). Zhao *et al.* (10) (with commentary by Wool, Reardon, and Getz (11)) reported similar findings regarding the efficacy of administering apoA-I mimetics by the oral route despite having undetectable plasma levels of peptide after oral administration. They added HDL-like nanolipid particles containing a peptide mimetic of apoA-I, (which is not structurally related to the 6F peptide) to the drinking water of *Ldlr*^{-/-} mice fed a high-fat high-cholesterol diet and observed a dramatic reduction in aortic atherosclerosis. The reduction in aortic atherosclerosis after oral administration was similar to that obtained after injection of the particles (10, 11). Administering the particles by injection resulted in high plasma peptide levels, but when the peptide was given in the drinking water, despite the similar reduction in aortic atherosclerosis, the peptide could not be detected in plasma (10, 11).

The apoA-I mimetic peptide 4F is structurally related to 6F but not structurally related to the peptide used by Zhao *et al.* (10). The 4F peptide differs from 6F by having two fewer phenylalanine residues and is more water soluble than 6F. When 4F was administered to mice by the oral route or by subcutaneous injection, at equal doses there was a similar reduction in plasma serum amyloid A (SAA) levels, and a similar reduction in HDL inflammatory properties, despite peptide plasma levels that were ~1,000-fold higher after injection compared with after oral administration (12). In these experiments, the amount of peptide found in the feces was similar at each dose of 4F regardless of whether the peptide was administered by the oral route or by subcutaneous injection (12). It was concluded that the intestine was a major site of action for the peptide, regardless of the route of administration (12). Subsequently it was found that, after injection of 4F into the tail vein of mice, the peptide rapidly appeared in the lumen of the duodenum and jejunum at levels greater than that found in the liver and promoted transintestinal cholesterol efflux (13). Together these studies strongly suggested that oral apoA-I mimetic peptides act on the luminal side of enterocytes to reduce systemic inflammation. These studies, however, did not provide mechanistic insight into how the peptides could profoundly decrease systemic inflammation without being absorbed.

The mucous layers of the small and large intestines provide a critical interface between enterocytes and the bacteria rich lumen. In the colon, there are two mucous layers; the inner layer is dense and prevents bacteria from directly interacting with the enterocytes (14, 15). In contrast, the mucous layer in the small intestine is much less of a barrier to bacteria (16). Ermund *et al.* (16) concluded that, in the small intestine, instead of a physical barrier as is the case in the colon, separation of

bacteria from enterocytes is more dependent on an array of antibacterial peptides and proteins that are secreted into the mucus to regulate the number of bacteria and their interaction with the enterocytes.

The experiments reported here surprisingly demonstrate that WD contains lower levels of oxidized phospholipids compared with the chow diet. However, when WD was fed to *Ldlr*^{-/-} mice the content of reactive oxygen species (ROS) and oxidized phospholipids in jejunum mucus increased and the content of antibacterial peptides and proteins in jejunum mucus decreased compared with when the mice were fed the chow diet. As a consequence, dysbiosis, increased gut permeability, and systemic inflammation resulted from feeding WD. All of these changes were ameliorated by adding to WD a concentrate of transgenic tomatoes expressing the apoA-I mimetic peptide 6F (Tg6F). The experiments reported here also show that adding oxidized phospholipids *ex vivo* to jejunum from mice fed a chow diet reproduced the gene expression changes seen *in vivo* when *Ldlr*^{-/-} mice were fed WD, and these changes were prevented when 6F peptide was added *ex vivo* with the oxidized phospholipids. The data in this article identify an important role for oxidized phospholipids in the mucus of the jejunum in causing dysbiosis and systemic inflammation and provide strong evidence that the mechanism of action of oral apoA-I mimetic peptides in mice fed WD is to protect against the increased levels of oxidized phospholipids that are formed on this diet.

MATERIALS AND METHODS

Materials

Transgenic tomatoes expressing the 6F peptide and control transgenic tomatoes expressing a marker protein, (β -glucuronidase) were grown and freeze-dried at the University of California, Davis as previously described (1). The composition of the freeze-dried tomatoes has previously been reported (1). The freeze-dried tomatoes were shipped on dry ice to UCLA where a concentrate of the transgenic tomatoes expressing the 6F peptide (Tg6F) and a concentrate of the control transgenic tomatoes (EV), which express β -glucuronidase instead of the 6F peptide, were prepared as described (8). Table 1 shows the sources for ELISA assay kits and materials. Nontransgenic 6F peptide was synthesized as described previously (1). In *ex vivo* experiments, a control peptide with 18 amino acid residues that was biologically inactive in preventing sphingomyelinase-induced LDL aggregation (17) was used. Oxidized 1-palmitoyl-2-arachidonoyl-*sn*-glycero-3-phosphocholine (Ox-PAPC) was purchased from Avanti Polar Lipids (catalog #870604P). Unless otherwise stated, other materials were from previously cited sources (8).

Mice and diets

Ldlr^{-/-} mice (originally purchased from Jackson Laboratories on a C57BL/6J background) were from the breeding colony of the Department of Laboratory and Animal

TABLE 1. Source and details of ELISA kits used in accordance with manufacturer's instructions

Protein Assayed	Tissue Source	Tissue Dilution	Kit Source	Catalog #
ATOHI	Whole jejunum	1:100	Aviva System Biology	OKEH05889
ApoA-I	Jejunum mucus	1:20	Abcam	ab221440
	Mesenteric lymph	1:10		
	Plasma	1:10,000		
DLL4	Whole jejunum	1:2	Abcam	Ab213860
GF11	Whole jejunum	1:100	Abxexa	abx525156
IgA	Jejunum mucus	1:100	Abcam	ab157717
IL-22	Whole jejunum	1:2	Biologend	436307
IL-23	Whole jejunum	1:2	Biologend	433704
IL-36 γ	Whole jejunum	1:10	Aviva Systems Biology	OKEH03002
LBP	Jejunum mucus	1:10	Enzo Life Sciences	ALX-804-502-C100
	Mesenteric lymph	1:10	Jackson Immuno Research	315-035-0031
	Plasma	1:10		
Lysozyme	Jejunum mucus	1:10	Lifeome	E91193Mu-1
Mucin2	Jejunum mucus	1:100	Lifeome	E15065m-96
NOTCH2	Whole jejunum	1:2	Aviva Systems Biology	OKEH05163-96W
Osteopontin	Jejunum mucus	No dilution	Abcam	ab100734
REG3A	Jejunum mucus	No dilution	Lifeome	E94675Mu-1
REG3B	Jejunum mucus	No Dilution	Lifeome	E99541Mu-1
Surfactant A	Jejunum mucus	1:100	Lifespan Biosciences	LS-F4286-1

Medicine at the David Geffen School of Medicine at UCLA. Mice had unlimited access to standard mouse chow (Ralston Purina Rodent Laboratory Chow catalog #5001; 4.5% fat by weight) prior to the start of experiments. As described previously (8), to ensure that the mice ate all of their food, during the experiments the mice did not have unlimited access to food, as was the case prior to starting the experiment. During the 2 weeks when the mice were on the experimental diets, the mice were given precisely 4 g of diet per mouse each night (each cage contained 4 mice; each cage received 16 g of diet each night). When the mice were switched to a Western Diet (WD), it was from Teklad, Harlan, (catalog #TD88137; 21.2% fat by weight). Tg6F or EV was added to WD at 0.06% by weight of diet as described (8). In each experiment, the mice received one of four diets for 2 weeks. One group continued on chow. A 2nd group was switched from chow to WD. A 3rd group was switched from chow to WD plus the EV control (WD + EV). The 4th group was switched from chow to WD plus Tg6F (WD + Tg6F). The dose of 6F peptide was 6.9 mg/kg/day for mice receiving WD + Tg6F. After receiving the diets for 2 weeks, all four groups gained weight. Mice receiving WD or WD + EV had greater weight gain compared with chow. Despite eating the same amount of WD each day, the mice receiving WD + Tg6F had significantly less weight gain compared with those receiving WD or WD + Tg6F (supplemental Fig. S1). This experimental design assured that all of the mice ate the same amount of food each day and that all four groups gained weight over the course of the 2 weeks indicating that the caloric intake even on the chow diet was sufficient. The gender and number of mice in each group is stated in the figure legends or in a supplemental table. If the age range did not exceed 1 month (e.g., age 2–3 months), only the age range of the mice is stated. If the age range of the mice used in the experiment exceeded 1 month, the mean \pm SEM of the group's age in months is reported. In each experiment, the number of mice of each age was the same for each of the four-diet groups. For example, if there were 16 mice per group with ages ranging between 4 and 7 months, there could be 4 mice age 4 months, 4 mice age 5 months, 4 mice age 6 months and 4 mice age 7 months in each of the four diet groups. In this example, the age of the mice would be stated as 5.5 \pm 0.3 months. The UCLA Animal Research Committee approved all experiments prior to initiation of the study, and the UCLA Division of Laboratory Animal

Medicine monitored the mice daily to ensure compliance with all applicable rules and regulations.

Tissue and cell collection

Collecting jejunum mucus and isolation of enterocytes from the same segment of jejunum. Mice were euthanized using isoflurane immediately prior to removing the small intestine. The small intestine was washed twice by flushing gently with ice-cold phosphate buffered saline (PBS). The duodenum was removed, and the following ~14 cm of jejunum was carefully opened longitudinally and pinned at the edge of one side using a supportive Styrofoam base. Any residual luminal content was removed by another gentle wash with PBS. The gelatinous mucosal surface was washed with 2 ml of a solution containing 10 mM Tris-HCl; pH 7.4 and 5 mM CaCl₂. The gelatinous mucosal surface was then scraped gently with a disposable cell lifter (Fisher Scientific Catalog #08-100-240). The gelatinous material was transferred from the cell lifter into a 1.5 ml Eppendorf tube containing 500 μ l of lysis buffer [50 mM Tris pH 7.5, 100 mM NaCl, 5 mM EDTA, 50 mM Na-orthovanadate, 1% Triton X-100, and one protease inhibitor tablet (Sigma-Aldrich Catalog #04693159001)] and was centrifuged for 10 min at 13,000 rpm to remove debris. The supernatant was transferred to another tube and centrifuged again for 10 min at 13,000 rpm. This supernatant was transferred to a new tube, and protein content was determined using the Bradford assay; absorbance was measured at 595 nm before storing the samples at -20° C. Prior to the addition of the lysis buffer, the gelatinous material contained few cells as shown by DAPI staining (~100 cells/ml) compared with enterocytes isolated from the same segment (~1.6 \times 10⁷ cells/ml), which were isolated as previously described (6).

Collecting mesenteric lymph. The method used was a modification of methods described previously (18, 19). To stimulate lymph flow and to facilitate identification of the mesenteric lymphatics draining the jejunum, 200 μ l of Kroger heavy whipping cream (refrigerated and used within 24 h of purchase) was administered to each mouse by stomach gavage. Two hours later, under isoflurane anesthesia, the abdomen was opened. The mesenteric lymphatics were identified by their white lucent color. Using a single-edge razor blade

(Fisher Scientific, Catalog #12-640) a mesenteric lymphatic vessel immediately adjacent to the jejunum was incised and Whatman Grade 3MM Chr Cellulose Chromatography Paper (Sigma-Aldrich catalog #3030917) was inserted into the incised lymph vessel to allow the lymphatic fluid to be absorbed. The paper was removed and transferred to a 1.5 ml Eppendorf tube containing 1 ml of methanol (Fisher Scientific Catalog #A456-4) and was placed on ice for 10 min. The tube was vortexed for 1 min, the paper was removed, and the tube contents were dried under argon gas, after which 250 μ l of PBS was added and the tube was vortexed for 1 min prior to distributing aliquots of the sample and storing them at -20°C .

Collecting adipose tissue. Epididymal adipose tissue was collected as described (20).

Ex vivo studies of jejunum

After an overnight fast, the intestines of *Ldlr*^{-/-} mice on a chow diet were gently washed with cold PBS being careful to avoid perforation. The jejunum was isolated and carefully cut into 2 cm sections. The jejunum sections were cut open and added to tubes containing 1 ml of PBS or 1 ml of PBS with 25 μ g of Ox-PAPC with or without 25 μ g of 6F peptide or the control peptide. The tubes were incubated at 37°C for 4 h with gentle mixing on a nutating mixer. The tubes were centrifuged at 13,000 rpm at 4°C for 5 min. The supernatant was carefully aspirated, the tissue was homogenized for 15 s, and RNA was isolated for RT-qPCR as described below.

Assays

Determination of oxidized phospholipids in jejunum mucus. Oxidized phospholipids were determined in jejunum mucus using an ELISA with the E06 antibody (Avanti Polar Lipids, catalog #33001S), a PC-BSA standard (Bioscience Technologies, catalog #PC-1011-10), and a 1:10 dilution as described previously (5).

Determination of nonoxidized lipids in jejunum mucus. Jejunum mucus lipids were extracted and analyzed at the UCLA Lipidomics Core by direct infusion shotgun mass spectrometry utilizing the Sciex Lipidizer Platform (21).

Determination of intestinal fat absorption. Intestinal fat absorption was measured by a modification of a previously published method (22).

Determination of reactive oxygen species in jejunum mucus. DCFH-DA (dichlorofluorescein; Thermo Fischer Scientific, catalog #D-399) was dissolved in fresh methanol at 2.0 mg/ml, vortexed 2 min, and incubated at room temperature for 30 min (protected from light) to release DCFH. On interaction with lipid oxidation products DCFH forms DCF, which produces intense fluorescence. Ten microliters of mucous material and 1x PBS were incubated for 30 min in a 37°C incubator. A volume of 500 μ l of DCFH was dried under argon, suspended in 5 ml of 1x PBS, and vortexed for 2 min to make a working stock of 200 μ g/ml. A volume of 25 μ l of the 200 μ g/ml stock solution was added per well and incubated (1 h) in a 37°C incubator. Fluorescence intensity was determined with a scanning Spectra Max Gemini XS Fluorescence plate reader set at an excitation wavelength of 485 nm and an emission wavelength of 530 nm. The fluorescence values were normalized to protein concentration.

Determination of gut permeability. After a 4 h fast, the mice were weighed. Fluorescein-5-isothiocyanate (FITC)-dextran (Sigma-Aldrich, catalog #FD4-1G) was dissolved in PBS and administered to each mouse by stomach gavage at 44 mg/100 g of body weight. Control mice received 200 μ l of PBS. Water bottles were removed immediately after gavage. Four hours after gavage, blood was collected by retro-orbital bleeding into a plasma collection tube (Fisher Scientific, catalog #02-675-187). The tube was centrifuged for 3 min at 15,000 g and plasma was collected. A standard curve was prepared by serially diluting FITC-dextran to the following concentrations: 0, 125, 250, 500, 1,000, 2,000, 4,000, and 8,000 ng/ml. Plasma was diluted with PBS at a dilution of 1:4 and measured in duplicate samples. Background subtraction was performed using plasma from mice that did not receive FITC-dextran. Filter settings were 485 nm for excitation and 520 nm for emission. Fluorescence intensity was measured in a Spectra Max Gemini XS Fluorescence plate reader. Fluorescence readings were normalized to protein concentration.

Isolation of RNA and gene expression analysis. Total RNA was isolated from mouse enterocytes or from whole jejunum or from jejunum segments using a Qiagen RNA extraction kit (catalog #74106) according to the manufacturer's instructions. The yield and purity of the isolated RNA was determined using a Nano-Drop spectrophotometer. Samples for real-time qPCR (RT-qPCR) had A260/A280 ratios between 1.9 and 2.05. First-strand cDNA was synthesized from 1 μ g of total RNA using a cDNA synthesis kit (Bio-Rad, catalog #1708890). The cDNA was diluted 1:10 with nuclease-free water. RT-qPCR was performed on a Bio-Rad CFX96 real-time PCR detection system using SYBR Green Supermix (Bio-Rad, catalog #1708880). Relative abundance of mRNA was calculated by normalizing to glyceraldehyde 3-phosphate dehydrogenase (GAPDH). Primer sequences are shown in supplemental Table S1.

Determination of proteins in jejunum mucus, whole jejunum, mesenteric lymph, and plasma. Protein levels in jejunum mucus were determined for ApoA-I, IgA, lipopolysaccharide binding protein (LBP), lysozyme, mucin2, osteopontin, regenerating islet-derived family members 3A (REG3A) and 3B (REG3B), and surfactant A. Protein levels in whole jejunum were determined for atonal homolog 1 (ATOH1), growth factor independent protein 1 (GF1I), IL-36 γ , IL-23, IL-22, NOTCH2, and DLL4. Protein levels in mesenteric lymph and in plasma were determined for ApoA-I and LBP. The levels of these proteins were determined by ELISA using kits according to the instructions of the manufacturer as shown in Table 1.

16S rRNA sequencing. DNA extraction and sequencing of the 16S ribosomal RNA gene was performed for jejunum mucus samples as described previously (23). In brief, bacterial DNA was extracted using a kit (ZymoBIOMICS, catalog #D4300) with bead beating. The V4 region of the 16S gene was amplified and barcoded using 515f/806r primers then 250x2 bp sequencing was performed on an Illumina NovaSeq 6000 system. DADA2 was used to perform quality-filtering (451,039 reads per sample) and assign reads to amplicon sequence variants, with taxonomy based on the Silva database (24).

Quantitative 16S and Akkermansia muciniphila PCR. Bacterial DNA was extracted using a kit (ZymoBIOMICS, catalog #D4300) with bead beating. The total number of copies of the

bacterial 16S rRNA gene was determined by a TaqMan-based quantitative PCR (qPCR) approach using previously published universal primers (25). The primer set included the forward primer, 5'-TCCTACGGAGGCAGCAGT-3'; the reverse primer, 5'-GGACTACCGGATCTAATCCTGTT-3'; and the probe, (6-carboxyfluorescein)-5'-CGTATTACCGC GGCTGCTGGCAC-3'-(carboxytetramethyl-rhodamine). *A. muciniphila* - Forward 5'AGA GGT CTC AAG CGT TGT TCG GAA-3'; *A. muciniphila* - Reverse 5'TTT CGC TCC CCT GGC CTT CGT GC-3'.

Using 5 µl of an iTaq Universal Probes Supermix (Bio-Rad, catalog # 1725131), 0.2 µM of forward and reverse primers, 0.25 µM of probe, 1 µl of sample DNA, and PCR-grade water, a total volume of 20 µl was used for each qPCR reaction. All samples were run in duplicate, and a stock *Escherichia coli* sample of a known quantity (1.7×10^{10} colony-forming units) was used to create a standard dilution curve for 16S rRNA. *A. muciniphila* standard curve was made from microbial DNA standard (Sigma-Aldrich, catalog #MBD001). The PCR reaction was performed using a Bio-Rad CFX384 or Bio-Rad CFX96 Touch Real-Time PCR Detection System. The reaction conditions for amplification of DNA were 50°C for 2 min, 95°C for 10 min, and 40 cycles of 95°C for 15 s and 60°C for 1 min. A linear regression model was fitted to threshold cycle values of the dilution curve and then used to determine the number of copies of the 16S rRNA gene present in each sample.

Immunohistochemistry. Fresh jejunum tissues (1 cm in length) were carefully excised, placed into a precooled (on dry ice) OCT containing cassette (Fisher Scientific Catalog # NC1466760), and stored at -80°C. The UCLA Pathology Core Facility prepared 5 µm thick tissue sections, which were thawed at room temperature for ~30 min before staining. The sections were fixed with 4% PFA for 10 min and washed with IX PBS. Blocking buffer was prepared with 10% BSA in IX PBST (IX PBS with 0.1% TritonX-100) and was added to the slides and incubated at room temperature for 90 min. Primary antibodies for mucin 2 (MUC2) (Santa Cruz Biotechnology, Catalog # sc15334), E-Cadherin (R&D systems, Catalog# AF748), and Lysozyme (Invitrogen, Catalog# PA5-16668) were added (1:200 dilution) to the sections in blocking buffer and incubated overnight at 4°C. The slides were washed twice with IX PBS and then stained with secondary antibodies (Invitrogen, Catalog # A32814 and Catalog # A10042) and with DAPI (Invitrogen, Catalog #D1306) for 90 min at room temperature. The slides were washed twice with IX PBS followed by addition of mounting solution (ThermoFisher, Catalog # P36931) and a coverslip. The negative control omitted the primary antibodies. Images were captured with 10× objective on a Zeiss LSM880 confocal microscope with ZEN software (Carl Zeiss Microscopy) for acquisition. MUC2-positive goblet cells were counted by evaluating 28 crypt-villus units per mouse (n = 3 mice/group) and Lysozyme-positive cells per crypt were counted by evaluating 40 crypts per mouse (n = 3 mice/group).

Other assays. Lymph and plasma lipids were determined as previously described (8). LPS in lymph and plasma was determined using a LAL Chromogenic Endotoxin Quantitation Kit (Thermo Fisher Scientific Pierce, catalog #88282) following the manufacturer's instructions. Plasma levels of IL-6 and SAA were determined as described previously (5).

Statistical analyses

For studies using the 16S sequencing method, alpha diversity was assessed by the Chaol index of microbial richness

and the significance of differences was calculated by Kruskal-Wallis with post hoc "Dunn's multiple comparison test." Beta diversity was calculated using square root Jensen-Shannon divergence and visualized by principal coordinates analysis. Significance was determined using multivariate Adonis in the R package vegan with batch as a covariate. Differential abundance of individual taxa was evaluated using DESeq2 in R, which employs an empirical Bayesian approach to shrink dispersion and fit nonrarefied count data to a negative binomial model (26). P-values for differential abundance were converted to q-values to correct for multiple hypothesis testing (<0.05 for significance) (27).

For other studies, in comparing more than two groups, ANOVA was performed and followed by multiple comparison tests using version 9.1.2 (GraphPad Software, San Diego, CA). Statistical significance was considered achieved if $P < 0.05$. Unless otherwise stated, values are presented as the mean ± SEM.

RESULTS

WD increased the number of bacteria and the content of LPS in jejunum mucus of *Ldlr*^{-/-} mice.

WD increased 16S rRNA copy numbers (Fig. 1A) and increased levels of LPS (Fig. 1B) in jejunum mucus. In each case, adding Tg6F (but not the EV control) to WD prevented the increase.

WD changed the microbiome, and *Akkermansia muciniphila* virtually disappeared from jejunum mucus of *Ldlr*^{-/-} mice.

Figure 2A demonstrates that the taxonomic composition of the bacteria in jejunum mucus at the phylum level was changed on feeding the mice WD compared with chow. Adding Tg6F to WD resulted in a taxonomic composition closer to chow compared with adding the EV control. Figure 2B demonstrates that the taxonomic composition of the bacteria in jejunum mucus at the

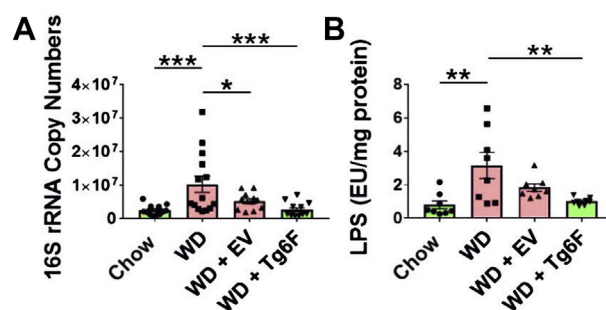


Fig. 1. Feeding *Ldlr*^{-/-} mice a Western diet (WD) increased 16S rRNA copy numbers and LPS levels in jejunum mucus. Adding a concentrate of control transgenic tomatoes (EV) to WD did not prevent the increase, but adding a concentrate of transgenic tomatoes expressing the 6F peptide (Tg6F) to WD prevented the increase. Female (A) or male (B) *Ldlr*^{-/-} mice aged 5–5.5 months (n = 14 mice per group) (A) or 3.5–4 months (n = 8 mice per group) (B) were fed the four diets and 16S rRNA copy numbers (A) were determined in mucus samples containing the same amount of DNA (50 ng) from each mouse or LPS (B) was determined in the mucus as described in [Materials and methods](#). * $P < 0.05$; ** $P < 0.01$; *** $P < 0.001$.

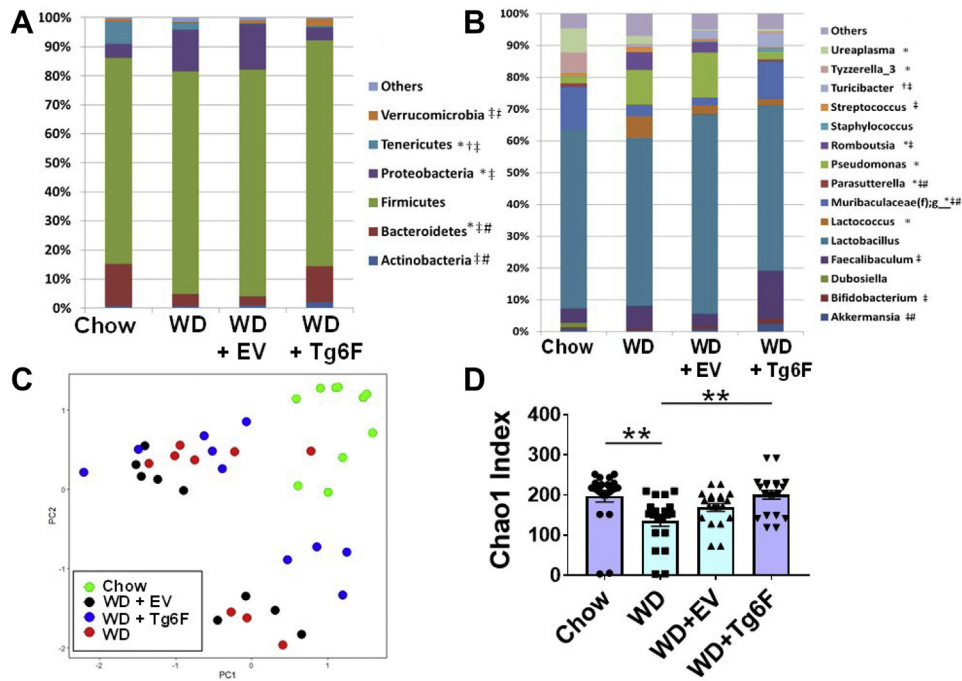


Fig. 2. Feeding *Ldlr*^{-/-} mice a Western diet (WD) changed the microbiome in jejunum mucus. A: At the phylum level, feeding *Ldlr*^{-/-} mice WD changed the taxonomic composition of the bacteria in jejunum mucus compared with chow. Adding a concentrate of transgenic tomatoes expressing the 6F peptide (Tg6F) to WD maintained the taxonomic composition closer to chow compared with adding a concentrate of control transgenic tomatoes (EV). Female *Ldlr*^{-/-} mice aged 4.8 ± 0.1 months (n = 10 mice per group) were fed the four diets and taxonomic composition at the phylum level was determined in the mucus as described in [Materials and methods](#). Significance of differences across groups was determined by DESeq2 analysis as described in [Materials and methods](#): *WD versus chow; †WD versus EV; ‡WD versus Tg6F; #EV versus Tg6F. B: The taxonomic composition at the genus level was determined in the jejunum mucus as described in [Materials and methods](#) for the mice described in (A). Significance of differences across groups was determined by DESeq2 analysis as described in [Materials and methods](#): *WD versus chow; †WD versus EV; ‡WD versus Tg6F; #EV versus Tg6F. C: Beta diversity analysis demonstrated that feeding *Ldlr*^{-/-} mice WD resulted in distinct microbial profiles in jejunum mucus compared with chow. Using the Adonis test, the differences across all four groups was significant ($P < 0.0001$), and there was a significant difference in microbial composition between WD + EV compared with WD + Tg6F ($P = 0.012$). Beta-diversity in jejunum mucus was determined as described in [Materials and methods](#). The groups in (A) comprised six female mice aged 4.5–5.5 months, and in a 2nd experiment four female mice aged 4.0–5.0 months. The data from the two experiments were combined and beta diversity analyses were adjusted for each experiment as a covariate as described in [Materials and methods](#). D: Alpha diversity in jejunum mucus was determined using the Chao1 index as described in [Materials and methods](#). ** $P < 0.01$.

genus level was also changed by feeding the mice WD compared with chow. Adding Tg6F to WD resulted in a taxonomic composition closer to chow compared with adding the EV control. [Figure 2C](#) presents the beta-diversity (28) for the bacteria in the jejunum mucus on the four diets. WD resulted in distinct microbial profiles in jejunum mucus compared with chow; this difference was reduced by adding Tg6F to WD. [Figure 2D](#) shows reduced alpha-diversity using the Chao1 index (29) in jejunum mucus on WD compared with chow, which was ameliorated by adding EV or Tg6F to WD, with greater effect of Tg6F.

To confirm that our sampling strategy was successful in obtaining the microbiome from jejunum mucus, we sequenced the microbiome from jejunum lumen and compared it with the microbiome in jejunum mucus. As shown in [supplemental Fig. S2A](#), we found that across all four diet groups, jejunum mucus had a distinct microbiome composition by beta diversity analysis when compared with the microbiome in the lumen of

the jejunum ($P = 0.005$). To confirm that these microbiome differences followed previously reported patterns, we assessed the abundance of members of the Proteobacteria phylum, which contains aerotolerant microbes that are known to be enriched in the mucous layer compared with the lumen (30). As expected, Proteobacteria phylum was enriched in jejunum mucus compared with jejunum lumen across the dietary groups ([supplemental Fig. S2B](#)).

Adding Tg6F to WD compared with adding the EV control to WD resulted in an increase in the phylum Verrucomicrobia ([Fig. 2A](#)). The phylum Verrucomicrobia contains the genus *Akkermansia*, which increased when Tg6F (but not the EV control) was added to WD ([Fig. 2B](#)). *A. muciniphila* is an inhabitant of intestinal mucus deemed essential for maintaining a healthy mucous layer and providing protection from obesity, diabetes, and atherosclerosis in mouse models (31–37). *A. muciniphila* has also been shown to be important in humans (31, 38–43).

Figure 3A and **B** demonstrate that, on WD in male and female mice, respectively, *A. muciniphila* virtually disappeared from jejunum mucus; after adding Tg6F (but not the EV control) to WD, the difference compared with chow was not significant.

Ottman *et al.* (41) reported that administration of pasteurized *A. muciniphila* protected mice from body weight gain and protected them from increased adipose tissue mass on a high-fat diet. We found that addition of Tg6F (but not the EV control) to WD protected against body weight gain (supplemental Fig. S1). Therefore, we determined if Tg6F protected against increased adipose tissue mass on WD. As shown in supplemental Fig. S3, this was indeed the case. Depommier *et al.* (37) reported that protection from weight gain by administration of pasteurized *A. muciniphila* was not due to protection from increased fat absorption on the high-fat diet as determined by gene expression studies. We measured fat absorption using a more direct method and found that Tg6F protection against body weight gain and increased adipose tissue mass on WD was also not due to protection from increased fat absorption. As shown in supplemental Figs. S4–S6, fat absorption in mice fed WD versus WD + EV versus WD + Tg6F was not different. Thus, the ability of Tg6F to ameliorate the WD-mediated loss of *A. muciniphila* (Fig. 3) may explain the ability of Tg6F to protect against WD-mediated body weight gain and increased adipose tissue mass.

WD altered gene expression in jejunum for peptides and proteins secreted into the mucous layer that limit the number of bacteria in the mucous layer and/or regulate their interaction with enterocytes

Unlike the colon where the dense inner mucous layer separates bacteria from enterocytes, the small intestine

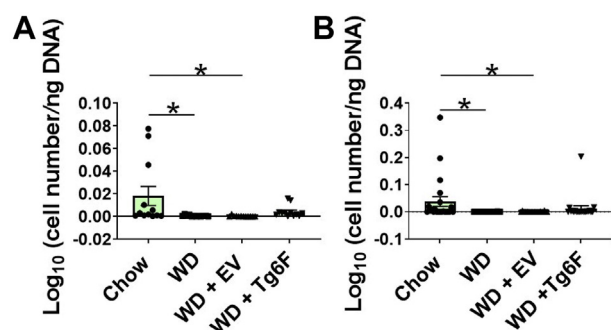


Fig. 3. *Akkermansia muciniphila* virtually disappeared from jejunum mucus when *Ldlr*^{-/-} mice were fed a Western diet (WD). Adding a concentrate of control transgenic tomatoes (EV) to WD did not ameliorate the loss, but after adding a concentrate of transgenic tomatoes expressing the 6F peptide (Tg6F) to WD, the difference compared with chow was not significant. Male (A) or female (B) *Ldlr*^{-/-} mice aged 4.3 ± 0.2 months (n = 12 mice per group) (A) or 5–5.5 months (n = 22 mice per group) (B) were fed the four diets and *Akkermansia muciniphila* was determined in the mucus by RT-qPCR as described in Materials and methods. *P < 0.05.

has a mucous layer that is less thick, less dense, and more porous (16). Consequently, the jejunum is much more dependent on antimicrobial peptides and proteins to protect the enterocytes from bacteria (16).

We selected 14 genes to study based on reports in the literature that their products limit the number of bacteria in intestinal mucus and/or regulate the interactions of intestinal bacteria with enterocytes. The data in Fig. 4 are presented as a heat map. For 12 of the 14 genes, the heat map appears to show decreased expression when the mice were fed WD compared with chow. For 10 of these 12 genes, the decrease reached statistical significance; there were two cases with P values of 0.0531 and 0.0654 (supplemental Table S2). For 11 of these 12 genes, adding Tg6F to WD resulted in gene expression that was equal to or greater than in mice fed chow; in one case it was less than chow (supplemental Table S2). For 11 of these 12 genes, adding Tg6F to WD resulted in gene expression that was greater compared with adding the EV control to WD. (supplemental Table S2). Two of the 14 genes studied showed increased expression compared with chow when the mice were fed WD with the EV control added, but the increased expression was prevented when Tg6F was added to WD (supplemental Table S2).

We previously reported that adding the 6F peptide to WD or adding the 6F peptide to wild-type tomato homogenate in WD gave the same results as adding transgenic tomatoes expressing the 6F peptide to WD (1). To rule out the possibility that the difference between the EV control and Tg6F was due to factors other than the 6F peptide, we compared WD + EV with WD + EV to which chemically synthesized 6F peptide was added at a dose equal to that obtained when Tg6F was added to WD (6.9 mg/kg/day of the 6F peptide). As shown in supplemental Fig. S7, the results are consistent with our prior results (1) and demonstrate that the differences between EV and Tg6F are due to the 6F peptide in the latter.

Regenerating islet-derived 3 genes (*Reg3a*, *Reg3b*, and *Reg3g*) (Fig. 4A) encode a family of proteins synthesized and secreted from Paneth cells in the intestine that play a major role in regulating the microbiota of the intestine (44–49).

The defensins (Fig. 4A) are antimicrobial peptides synthesized and secreted by Paneth cells in the intestine (50–53).

Lysozyme (*Lyz*) (Fig. 4A) is a major component of the antimicrobial defense in the intestine. It is also synthesized and secreted by Paneth cells in the intestine (54).

Intestinal alkaline phosphatase (*Alp1*) (Fig. 4A) is synthesized by enterocytes, stored in their brush border, and upon release has the ability to detoxify LPS and prevent bacterial invasion across the gut mucosal barrier (55, 56).

Deleted in malignant brain tumor 1 (*Dmbt1*) (Fig. 4A) has the capacity to agglutinate several gram-negative and gram-positive bacteria and, in concert with

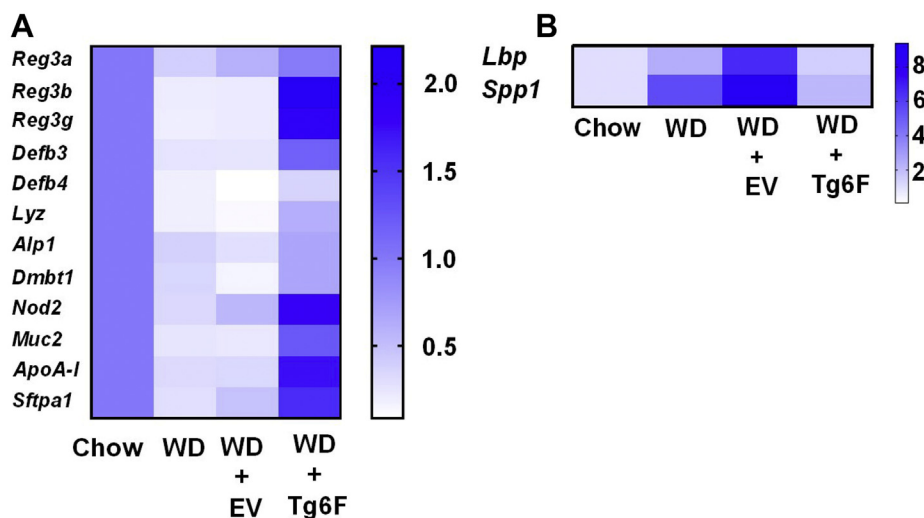


Fig. 4. Fourteen genes were selected for study based on reports in the literature that their products limit the number of bacteria in intestinal mucus and/or regulate the interactions of intestinal bacteria with enterocytes. Gene expression in the jejunum for these 14 genes was determined by RT-qPCR as described in [Materials and methods](#). The data are presented as a heat map, which compares expression of each gene on WD or WD + EV or WD + Tg6 with Chow. A: Shows 12 genes that appear to decrease on WD or WD + EV. B: Shows 2 genes that appear to increase on WD or WD + EV. [Supplemental Table S2](#) contains the experimental details for each gene.

surfactant proteins, can agglutinate virus particles (57) and is upregulated by IL-22 in intestinal cells (58). *Dmbt1* is also regulated by nucleotide-binding oligomerization domain-containing 2 (*Nod2*) (59) (Fig. 4A) and toll receptor 4.

Mucin 2 (*Muc2*) (Fig. 4A) is a major component of intestinal mucus that is synthesized and secreted by goblet cells (60); it binds bacteria in intestinal mucus (61).

ApoA-I (Fig. 4A) is synthesized and secreted by enterocytes in the small intestine and has antimicrobial properties that are in part due to its ability to bind LPS (62–64).

Surfactant A (*Sftpa1*) (Fig. 4A), which is synthesized and secreted by enterocytes (65, 66), inhibits the growth of gram-negative bacteria (67).

The protein product of *Lpb* (Fig. 4B) plays an important role in the response to LPS in the intestine. The major cell type producing LBP in the mouse small intestine was reported to be the Paneth cell (68), but intestinal epithelial cells can also produce LBP (69).

Osteopontin (also known as secreted phosphoprotein 1) is the protein product of the *Spp1* gene (Fig. 4B). Osteopontin has been shown to be important for intestinal intraepithelial lymphocyte regulation of the microbiota in mice (70, 71).

Confirmation of the gene expression data by ELISA

We were able to obtain reagents to allow us to quantify a number of the protein products of the genes shown in Fig. 4. [Figure 5A](#) shows the ELISA data for REG3A. [Figure 5B](#) shows the ELISA data for REG3B. [Figure 5C](#) shows the ELISA data for lysozyme.

[Figure 5D](#) shows the ELISA data for MUC2. [Figure 5E](#) shows the ELISA data for ApoA-I. [Figure 5F](#) shows the ELISA data for surfactant A. [Figure 5G](#) shows the ELISA data for LBP. [Figure 5H](#) shows the ELISA data for osteopontin. The proteins that we were able to test by ELISA confirmed the gene expression data in Fig. 4. However, not all antimicrobial agents secreted into jejunum mucus changed. As shown in [Fig. 5I](#), the content of IgA in jejunum mucus was not altered by any of the four diets.

WD altered the expression of genes that regulate the production and function of goblet and Paneth cells and the levels of antimicrobial peptides and proteins in intestine

We selected 10 genes to study based on reports in the literature that their products regulate the production and function of goblet and Paneth cells and the levels of antimicrobial peptides and proteins in the intestine. The data are presented as a heat map, which shows the expression of each gene when the mice were fed WD or WD + EV or WD + Tg6 compared with chow ([Fig. 6](#)). [Supplemental Table S4](#) shows the gender, age, number of mice per group, the source of the mRNA, and the *P* value for each WD containing diet (WD or WD + EV or WD + Tg6F) compared with chow for each gene in [Fig. 6](#).

IL-36 γ , IL-23, and IL-22 have been shown to be required for the expression of a number of genes shown in [Fig. 4](#) (72–76). [Figure 6](#) shows that the expression in jejunum of the genes for these interleukins (*Il36 γ* , *Il23*, and *Il22*, respectively) were decreased by WD, and the decrease was prevented by adding Tg6F to WD (but not the EV control).

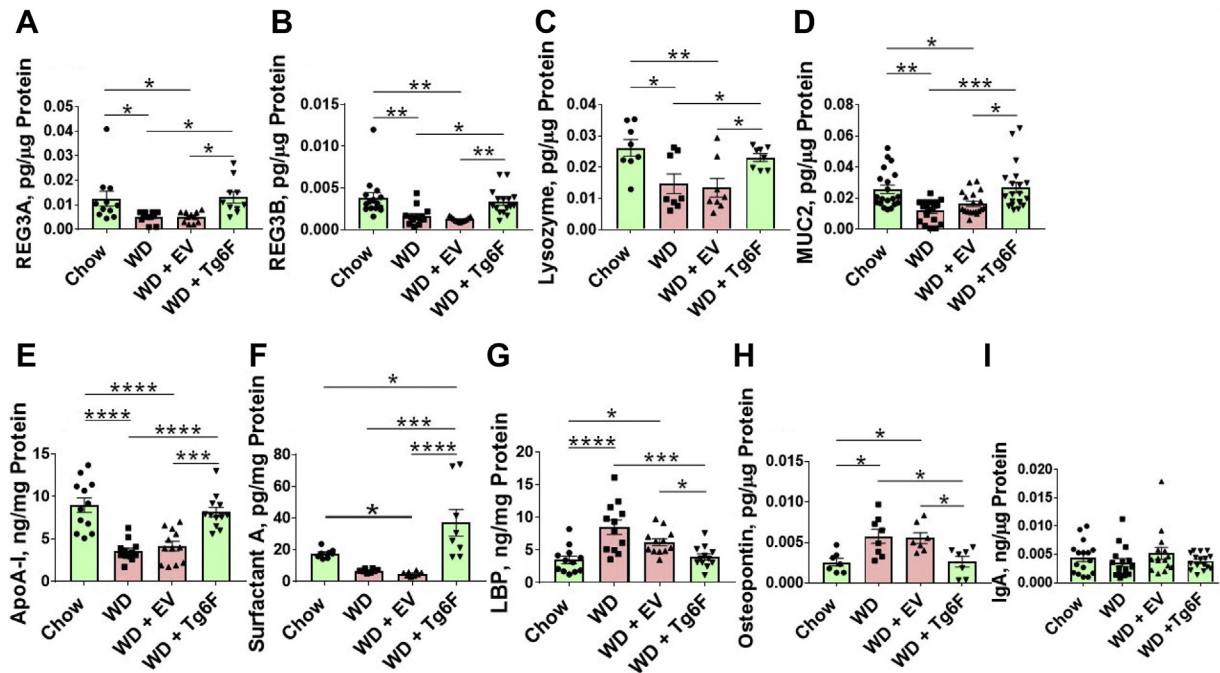


Fig. 5. ELISA confirms gene expression data in Fig. 4. *Ldlr*^{-/-} mice were fed the four diets, and the levels of protein in jejunum mucus (except for osteopontin, which was determined in whole jejunum) were determined by ELISA as described in [Materials and methods](#). The gender, age, and number of mice per group for each protein are shown in [supplemental Table S3](#). A: Regenerating islet-derived family member 3 alpha (REG3A). B: Regenerating islet-derived family member 3 beta (REG3B). C: Lysozyme. D: Mucin 2 (MUC2). E: ApoA-I. F: Surfactant A. G: LPS-binding protein (LBP). H: Osteopontin. I: Immunoglobulin A (IgA). **P* < 0.05; ***P* < 0.01; ****P* < 0.001; *****P* < 0.0001.

Ngo *et al.* (75) reported that *Il36γ*-induced *Il23* expression was highly dependent on *Notch2*. Figure 6 shows that the expression of *Notch2* was decreased by feeding the mice WD or WD + EV compared with

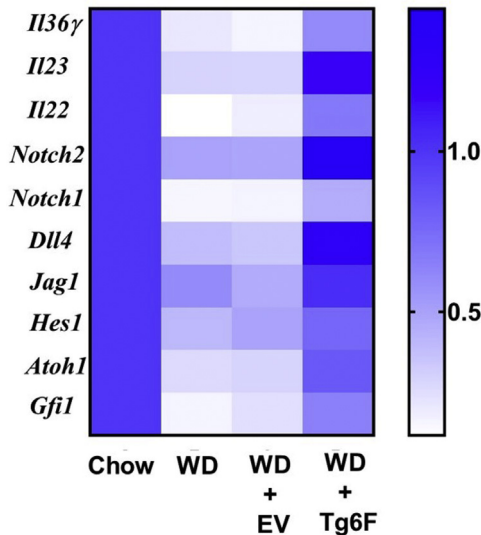


Fig. 6. Ten genes were selected for study based on reports in the literature that their products regulate the production and function of goblet and Paneth cells and the levels of antimicrobial peptides and proteins in the intestine. Gene expression in the jejunum for these 10 genes was determined by RT-qPCR as described in [Materials and methods](#). The data are presented as a heat map, which compares expression of each gene on WD or WD + EV or WD + Tg6F with Chow. [Supplemental Table S4](#) contains the experimental details for each gene.

feeding the mice WD + Tg6F, which was not different from feeding the mice chow.

Bohin *et al.* (77) reported that loss of Notch signaling led to Paneth cell apoptosis, which would be expected to lead to a decrease in a number of antimicrobial peptides and proteins shown in Figs. 4 and 5. Figure 6 shows that gene expression of *Notch1* was also decreased by WD, and the decrease was partially prevented by adding Tg6F to WD (but not the EV control). Figure 6 shows similar gene expression for the Notch target genes *Dll4*, *Jag1*, and *Hes1* on the four diets. Deficiency of *Hes1* was reported to cause dysbiosis (61).

The formation of functional goblet and Paneth cells requires the basic helix-loop-helix transcription factor atonal homolog 1 (*Atoh1*) also known as *Math1* (78–80). The expression of *Atoh1* was decreased by WD, and the decrease was prevented by adding Tg6F to WD (but not the EV control) (Fig. 6). Growth factor independent protein 1 (*Gfi1*), a zinc-finger protein family member, is a direct target gene of *Atoh1* and is required for the formation of Paneth cells (80, 81), and together with an ETS transcription factor (SPDEF) is required for goblet cell formation (82). Figure 6 demonstrates that expression of *Gfi1* on the four diets was similar to that for *Atoh1*.

ELISA and immunohistochemistry confirm gene expression data

Consistent with the gene expression data in Figs. 6 and 7A–C show the ELISA data for IL-36γ, IL-23, and

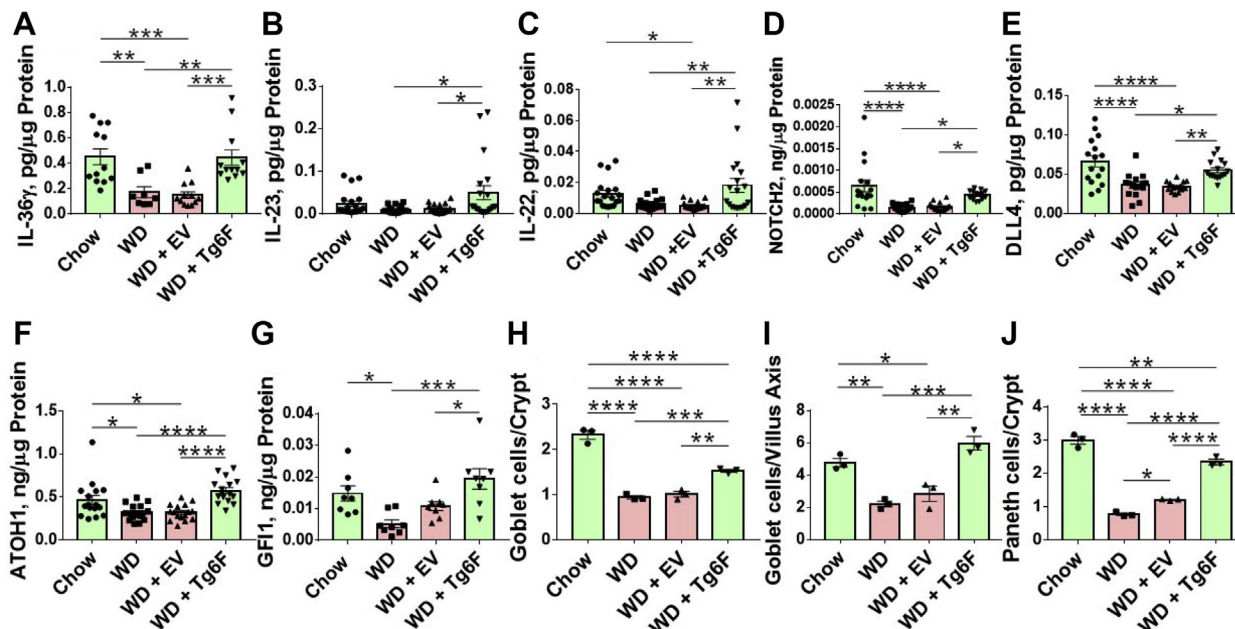


Fig. 7. ELISA and immunohistochemistry confirm gene expression data in Fig. 6. *Ldlr*^{-/-} mice were fed the four diets, and the levels of protein in jejunum were determined by ELISA or the number of goblet cells or Paneth cells in jejunum were determined by immunohistochemistry as described in Materials and methods. The gender, age, and number of mice per group for each panel are shown in supplemental Table S5. A: IL-36 γ . B: IL-23. C: IL-22. D: NOTCH2. E: DLL4. F: ATOH1. G: GFII1. H: Goblet cells/crypt. I: Goblet cells/villus axis. J: Paneth cells/crypt. **P* < 0.05; ***P* < 0.01; ****P* < 0.001; *****P* < 0.0001.

IL-22, respectively. Figure 7D and E show the ELISA data for NOTCH2 and DLL4, respectively. Figure 7F and G show the ELISA data for ATOH1 and GFII1, respectively. Consistent with the gene expression data, by immunohistochemistry, WD caused a decrease in the number of goblet cells (Fig. 7H and I), and Paneth cells (Fig. 7J) in jejunum, and the decrease was largely prevented by adding Tg6F to WD (but not the EV control).

WD increased oxidized phospholipids and ROS in jejunum mucus

The data in Fig. 8A demonstrate that WD increased the content of oxidized phospholipids in jejunum mucus, which was prevented by adding Tg6F to WD (but not the EV control). One might expect WD to have a high level of oxidized phospholipids compared with the chow diet or the WD + Tg6F diet. However, this was not the case. Indeed, the oxidized phospholipid content in the chow diet was the highest of the four diets (supplemental Fig. S8A). The mice in Fig. 8A were female; male mice showed similar results (supplemental Fig. S8B).

Lipidomics analysis of nonoxidized phospholipids in jejunum mucus revealed that, compared with the chow diet, feeding WD resulted in increased levels of nonoxidized phosphatidylcholine (supplemental Fig. S9A), nonoxidized phosphatidylethanolamine (supplemental Fig. S9B), and nonoxidized phosphatidylinositol (supplemental Fig. S9C), but in each case and in contrast to the case for oxidized phospholipids, there was no difference in the levels of these nonoxidized

phospholipids in the mice fed WD versus WD + EV versus WD + Tg6F. In addition, there was no difference in the levels of nonoxidized phosphatidylserine in jejunum mucus from mice on any of the four diets (supplemental Fig. S9D). The results in Fig. 8A and in supplemental Figs. S8 and S9 indicate that the increased content of oxidized phospholipids in jejunum mucus of the mice fed WD was due to the digestion and metabolism of WD, and was not due to the content of oxidized or nonoxidized phospholipids in WD prior to feeding WD to the mice.

Feeding WD to *Ldlr*^{-/-} mice also resulted in increased levels of ROS in jejunum mucus (Fig. 8B), which was prevented by adding Tg6F to WD (but not the EV control). The mice in Fig. 8B were female; male mice showed similar results (supplemental Fig. S8C).

WD increased gut permeability

Gut permeability is an important measure of the ability of the intestine to perform as a selective barrier. We previously reported that loss of this barrier function occurs earlier than signs of inflammation in mouse models of inflammatory bowel disease (9). However, in these studies, we did not determine if oral apoA-I mimetic therapy altered the changes in barrier function (9). As shown in Fig. 8C, feeding *Ldlr*^{-/-} mice WD for 2 weeks resulted in increased gut permeability that was prevented if Tg6F was added to WD (but not the EV control). Enterocyte gene expression was decreased on WD for claudin 4 (*Cldn4*) (Fig. 8D) and occludin (*Ocln*) (Fig. 8E), two genes known to be involved in tight

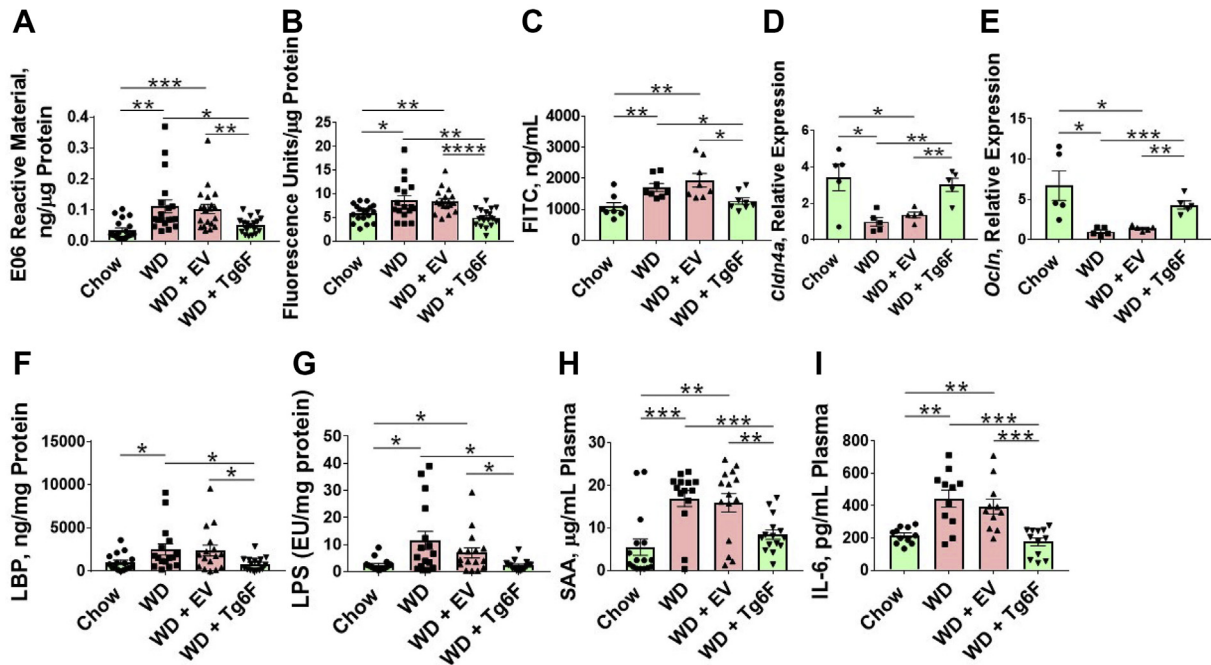


Fig. 8. Feeding *Ldlr*^{-/-} mice a Western diet (WD) increased the oxidized phospholipid and reactive oxygen species (ROS) content of jejunum mucus, increased gut permeability, decreased gene expression for tight junction proteins in jejunum enterocytes, increased LBP and LPS content of mesenteric lymph, and increased plasma levels of SAA and IL-6. Adding a concentrate of control transgenic tomatoes (EV) to WD did not prevent these changes, but adding a concentrate of transgenic tomatoes expressing the 6F peptide (Tg6F) to WD prevented the increase. The content of oxidized phospholipids (A) and ROS (B) was determined in jejunum mucus as described in [Materials and methods](#). Gut permeability (C) and gene expression in jejunum enterocytes for claudin4a (*Cldn4a*) (D) and occludin (*Ocln*) (E) were determined as described in [Materials and methods](#). LBP (F) and LPS (G) were measured in mesenteric lymph draining from jejunum as described in [Materials and methods](#). Levels of SAA (H) and IL-6 (I) were determined in plasma as described in [Materials and methods](#). The gender, age, and number of mice per group for each panel are shown in [supplemental Table S6](#). **P* < 0.05; ***P* < 0.01; ****P* < 0.001; *****P* < 0.0001.

junction formation (83, 84). Adding Tg6F to WD (but not the EV control) prevented the decrease.

WD increased LBP and LPS levels in mesenteric lymph draining the jejunum and in plasma

Based on the literature (69, 85, 86), and the increased levels of LBP and LPS in jejunum mucus on WD (Figs. 5G and 1B, respectively), we might expect to find increased levels of LBP and LPS in the mesenteric lymph draining the jejunum in mice fed WD. A common method to identify mesenteric lymph vessels employs the administration of a single dose of cream by stomach gavage 2 h prior to collecting lymph. This stimulates chylomicron formation and renders the mesenteric lymphatic vessels visible. The data in [supplemental Fig. S10A](#) and [B](#) demonstrate that after feeding the four diets for 2 weeks, administration of cream 2 h before sacrifice did not change the pattern of response to the four diets in jejunum enterocytes. Moreover, despite all groups receiving a single dose of cream by stomach gavage 2 h prior to lymph collection, the levels of lymph triglycerides, lymph total cholesterol, and lymph apoA-I still reflected the diet administered in the prior 2 weeks ([supplemental Fig. S11A–F](#)).

As expected, LBP was increased in mesenteric lymph from mice that received WD, but LBP levels were not

different from that of mice on chow when Tg6F was added to WD (Fig. 8F). LPS was similarly increased in mesenteric lymph from mice that received WD, but LPS levels were not different from that of mice on chow when Tg6F was added to WD (Fig. 8G). The mice in Fig. 8F and G were female. Male mice showed similar results ([supplemental Fig. S12A](#) and [B](#) for LBP and LPS, respectively). Plasma levels of LBP and LPS paralleled those in mesenteric lymph ([supplemental Fig. S12C–F](#)).

WD increased plasma markers of systemic inflammation

As shown in Fig. 8H and I, plasma levels of SAA and IL-6, respectively, were increased by WD, but the levels were not different from that of mice on chow when Tg6F was added to WD. The data shown in Fig. 8H and I were from male mice; female mice showed similar results ([supplemental Fig. S13A](#) and [B](#)).

Exposing jejunum to oxidized phospholipids ex vivo recapitulated gene expression changes in vivo

Figures 9–11 demonstrate that adding oxidized phospholipids ex vivo to jejunum from *Ldlr*^{-/-} mice on a chow diet reproduced the changes in gene expression in vivo that occurred when *Ldlr*^{-/-} mice were fed WD.

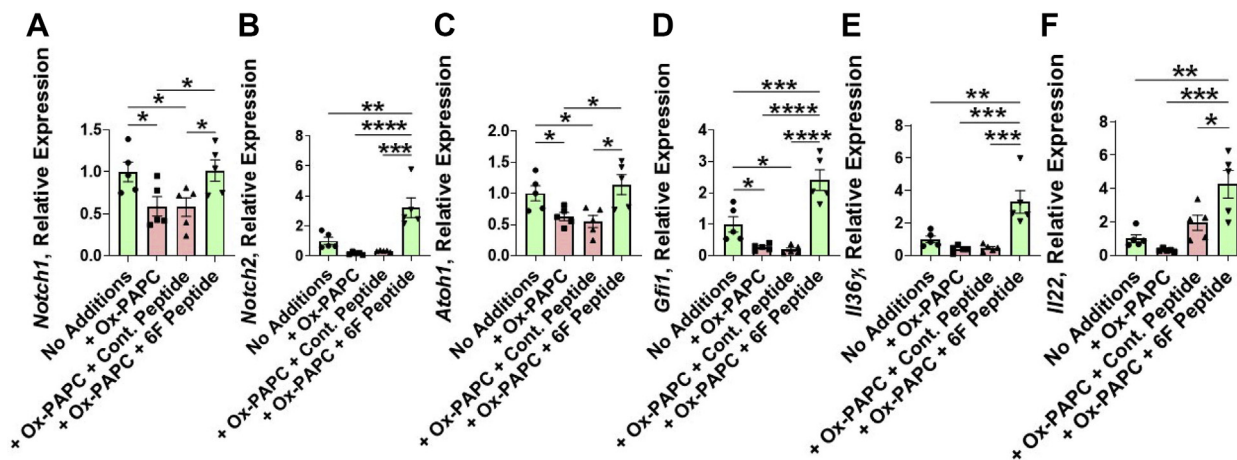


Fig. 9. Adding oxidized phospholipids ex vivo to jejunum from mice fed a chow diet reproduced the decrease in gene expression seen in jejunum from *Ldlr*^{-/-} mice fed WD for genes whose protein products regulate levels of antimicrobial peptides and proteins or are required for the formation of cells that produce these antimicrobial agents. Adding oxidized phospholipids together with chemically synthesized 6F peptide to jejunum ex vivo prevented the decrease, and in some cases increased gene expression above that seen in the absence of additions to the incubation. Jejunum segments from male *Ldlr*^{-/-} mice on a chow diet aged 3 months (n = 5 per group) were incubated with no additions, or with oxidized phospholipids (Ox-PAPC) or with Ox-PAPC together with a control (Cont.) peptide or with Ox-PAPC together with chemically synthesized 6F peptide as described in [Materials and methods](#). After 4 h of incubation gene expression was determined in the jejunum segments by RT-qPCR as described in [Materials and methods](#) for *Notch1* (A), *Notch2* (B), *Atoh1* (C), *Gfi1* (D), *Il36γ* (E), and *Il22* (F). **P* < 0.05; ***P* < 0.01; ****P* < 0.001; *****P* < 0.0001.

Figure 9 shows results for genes whose protein products regulate levels of antimicrobial peptides and proteins or are required for the formation of the cells that produce these antimicrobial agents in jejunum. Figure 9A shows the data for *Notch 1*, which encodes a signaling protein that is required to prevent Paneth cell apoptosis. Figure 9B shows the data for *Notch2*, which encodes a signaling protein that is required for IL-36 production. Figure 9C shows the data for *Atoh1*, which encodes a protein that is required for the formation of functional goblet and Paneth cells. Figure 9D shows the data for *Gfi1*, which encodes a protein required for the formation of functional Paneth cells. Figures 9E and F show the data for *Il36γ* and *Il22*, respectively, which encode the IL-36 and IL-22 proteins that are required for maintaining the levels of many antimicrobial proteins. Figures 10 and 11 show results for genes whose protein products limit bacterial numbers or regulate the interaction of bacteria with enterocytes. Figure 10A and B show the data for *Reg3b* and *Reg3g*, which encode important antimicrobial proteins. Figure 10C shows the data for *Alp1*, which encodes intestinal alkaline phosphatase that regulates LPS levels in the gut. Figure 10D–F show the data for the genes encoding apoA-I, surfactant A, and lysozyme, respectively, all of which have antimicrobial properties. Figure 11A shows the data for *Lbp*, which encodes the LPS-binding protein that increases in response to increased levels of LPS. Figure 11B shows the data for the gene encoding the osteopontin protein, which is required for intra-epithelial lymphocyte regulation of the microbiota. In every case in Figs. 9–11, adding oxidized phospholipids ex vivo to jejunum from mice on a chow diet resulted directionally in the same changes in gene expression

that were seen in vivo when the mice were fed WD. All of the 12 genes in Figs. 9 and 10 showed decreased expression upon addition of oxidized phospholipids ex vivo to jejunum from mice on a chow diet. All of these 12 genes showed decreased expression in jejunum in vivo when the mice were fed WD. The two genes in Fig. 11 showed increased expression upon addition of oxidized phospholipids ex vivo to jejunum from mice on a chow diet. Both of these genes showed increased expression in jejunum in vivo when the mice were fed WD. In every case except for one in Figs. 9–11, adding chemically synthesized 6F peptide together with the oxidized phospholipids prevented the ex vivo changes significantly better than the control peptide. Indeed, adding the 6F peptide often resulted in levels of gene expression that were significantly better compared with No Addition (e.g., in the case of genes with decreased expression on exposure to oxidized phospholipids, adding Tg6F with the oxidized phospholipids often resulted in higher values compared with No Addition). Figure 10F shows the data for a single exception in comparing the control peptide to the 6F peptide. In the case of lysozyme, adding oxidized phospholipids ex vivo significantly decreased the expression for the lysozyme gene in jejunum. However, adding either the control peptide or the 6F peptide prevented the decreased gene expression similarly. The implications of this isolated finding are considered in the Discussion section.

DISCUSSION

In a previous publication (2) we performed microarray analysis on whole jejunum from *Ldlr*^{-/-} mice fed

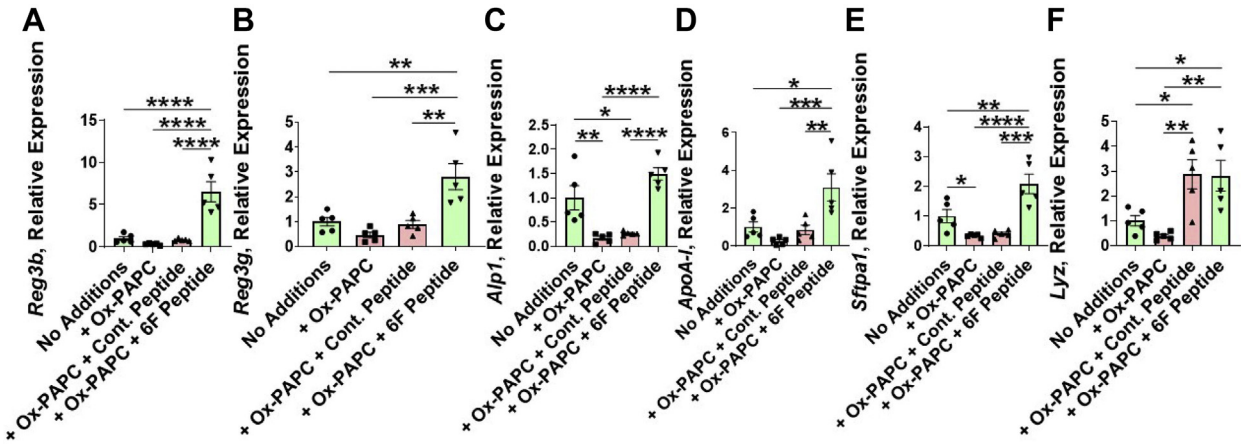


Fig. 10. Adding oxidized phospholipids ex vivo to jejunum from mice fed a chow diet reproduced the decrease in gene expression seen in jejunum from *Ldlr*^{-/-} mice fed WD for genes whose protein products limit bacteria numbers or regulate the interaction of bacteria with enterocytes. Adding oxidized phospholipids together with chemically synthesized 6F peptide to jejunum ex vivo prevented the decrease, and in some cases increased gene expression above that seen in the absence of additions to the incubation. Jejunum segments from the mice described in Fig. 9 were incubated with no additions, or with oxidized phospholipids (Ox-PAPC) or with Ox-PAPC together with a control (Cont.) peptide or with Ox-PAPC together with chemically synthesized 6F peptide as described in Materials and methods. After 4 h of incubation gene expression was determined in the jejunum segments by RT-qPCR as described in Materials and methods for *Reg3b* (A), *Reg3g* (B), *Alp1* (C), *ApoA-I* (D), *Sftpa1* (E), and *Lyz* (F). **P* < 0.05; ***P* < 0.01; ****P* < 0.001; *****P* < 0.0001.

chow or WD. There were 28 genes identified whose expression was significantly decreased on WD and 36 genes whose expression was significantly increased on

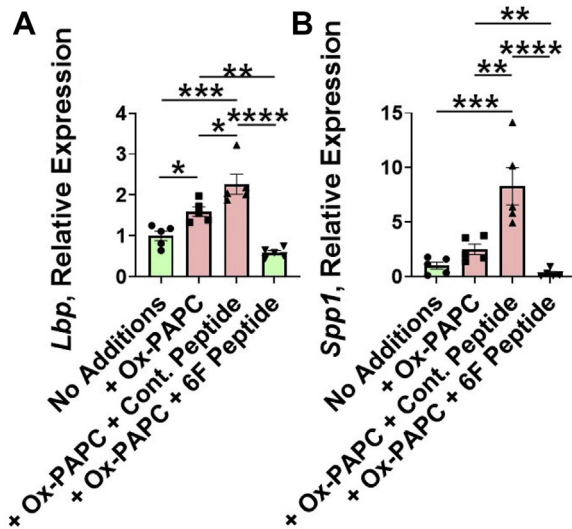


Fig. 11. Adding oxidized phospholipids ex vivo to jejunum from mice fed a chow diet reproduced the increase in gene expression seen in jejunum from *Ldlr*^{-/-} mice fed WD for two genes whose protein products limit bacteria numbers or regulate the interaction of bacteria with enterocytes. Adding oxidized phospholipids together with chemically synthesized 6F peptide to jejunum ex vivo prevented the increase. Jejunum segments from the mice described in Fig. 9 were incubated with no additions, or with oxidized phospholipids (Ox-PAPC) or with Ox-PAPC together with a control (Cont.) peptide or with Ox-PAPC together with chemically synthesized 6F peptide as described in Materials and methods. After 4 h of incubation gene expression was determined in the jejunum segments by RT-qPCR as described in Materials and methods for *Lbp* (A), and *Spp1* (B). **P* < 0.05; ***P* < 0.01; ****P* < 0.001; *****P* < 0.0001.

WD, and in each case the change was ameliorated by adding freeze-dried tomato powder to WD from transgenic tomatoes expressing the 6F peptide, but was not ameliorated by adding freeze-dried tomato powder to WD from control transgenic tomatoes (EV). Only 2 of these 64 genes (*Reg3b* and *Reg3g*) were involved in controlling bacterial proliferation or the interaction of bacteria with enterocytes (2). The vast majority of the genes identified by this microarray analysis were involved in lipid metabolism. In contrast, in the studies reported here, feeding WD to *Ldlr*^{-/-} mice resulted in a remarkable reduction in many (but not all) peptides and proteins that limit bacteria numbers in jejunum mucus and prevent their interaction with enterocytes. Why were not the gene expression changes reported here also seen in the previous microarray analysis? There are many possibilities including the fact that the previous studies were conducted with freeze-dried tomato powder added to WD, whereas in the current studies, we used a concentrate of the tomatoes that is much more potent than the freeze-dried preparations (4).

The changes reported here resulted in dysbiosis and the virtual elimination of *A. muciniphila* from jejunum mucus (Fig. 3), but with an increase in overall bacteria numbers (Fig. 1A), and increased levels of LPS in jejunum mucus (Fig. 1B). These changes in jejunum mucus were associated with increased gut permeability (Fig. 8C-E) and increased LPS levels in the lymph draining the jejunum (Fig. 8G and supplemental Fig. S12B) and in plasma (supplemental Fig. S12C-F).

We found several mechanisms that could explain these changes. WD decreased IL-36γ, IL-23, and IL-22 levels in jejunum (Fig. 7A-C, respectively). These

interleukins have been shown to control the levels of many antimicrobial peptides and proteins in the intestine (72–76). This may have resulted because WD decreased NOTCH2 in jejunum (Fig. 7D), which is required to maintain levels of IL-36 γ and IL-23 (75), which control the levels of IL-22 that is required to maintain the levels of many antimicrobial peptides and proteins in intestine. Future studies utilizing *Notch2* knockout mice could definitively test this hypothesis.

WD also decreased jejunum levels of the Notch target gene, *Hes1* (Fig. 6), which when deficient in mice leads to dysbiosis (61). Moreover, WD decreased the helix-loop-helix transcription factor *Atoh1* in jejunum (Figs. 6 and 7F) that is required for the formation of goblet cells and Paneth cells (78–80). In addition, WD decreased the expression of a direct target gene of *Atoh1*, the zinc-finger protein family member *Gfi1* (Figs. 6 and 7G), which is required for the formation of Paneth cells (80, 81). Consistent with these changes, WD decreased the number of goblet cells (Fig. 7H and I) and Paneth cells (Fig. 7J) in jejunum. Our findings in *Ldlr*^{-/-} mice regarding a decrease in jejunum goblet and Paneth cells on WD are consistent with the findings of Lee *et al.* (87) who found such changes in the small intestine of wild-type C57BL/6 mice that were fed a similar high-fat high-cholesterol diet.

Adding Tg6F to WD (but not the EV control) ameliorated these WD-mediated changes. What could be the mechanisms by which Tg6F partially or completely prevented all of the many changes reported in this manuscript? Our prior work in endothelial cells (88) demonstrated that oxidized phospholipids profoundly decreased Notch pathway signaling and led to increased inflammation. In the current studies, feeding WD resulted in a marked increase in oxidized phospholipids in jejunum mucus, and adding Tg6F to WD (but not the EV control) resulted in levels in jejunum mucus similar to that in chow-fed mice (Fig. 8A and supplemental Fig. S8B). The 6F peptide is one of three 18-amino-acid apoA-I mimetic class A amphipathic helical peptides that have the ability to bind oxidized lipids with such high affinity that the oxidized lipids are unable to interact with cells in the presence of the peptides (89). The three peptides 4F, 5F, and 6F have 4, 5, or 6 phenylalanine residues on the hydrophobic face of the peptide, respectively (89). The ability of these apoA-I mimetic peptides to bind oxidized phospholipids is many orders of magnitude greater than that of human apoA-I (90). Both the E06 antibody and the apoA-I mimetic peptide 4F block the activity of oxidized phospholipids in vitro and in vivo (91, 92). In addition, these apoA-I mimetic peptides were shown to bind and block oxidized phospholipid proinflammatory responses in human macrophages and intestinal epithelium and directly clear proinflammatory lipids from mouse intestinal tissue and plasma (9). Therefore, it is possible that Tg6F ameliorated the biological effects of the oxidized phospholipids in

jejunum mucus, because the 6F peptide bound the oxidized phospholipids with such high affinity that it prevented their interaction with the enterocytes, and promoted their destruction by the microbiota and/or their excretion in the feces.

Thus, it is possible that in the present studies many of the WD-mediated changes in jejunum were due to the increased content of oxidized phospholipids in jejunum mucus. The data in Figs. 9–11 strongly support that this is indeed the case since ex vivo exposure of jejunum from mice fed a chow diet to oxidized phospholipids resulted in gene expression that was remarkably similar to that seen in vivo when *Ldlr*^{-/-} mice were fed WD. In every case, gene expression that decreased in jejunum of mice fed WD decreased ex vivo upon addition of oxidized phospholipids to jejunum of mice fed a chow diet (Figs. 9 and 10). In both cases in which gene expression increased when the mice were fed WD, they also increased ex vivo upon addition of oxidized phospholipids (Fig. 11). With only one exception, adding the 6F peptide with oxidized phospholipids ex vivo ameliorated the changes better than a control peptide and often resulted in levels of gene expression that were better than that seen when oxidized phospholipids were not added to jejunum ex vivo (ie, compared with No Additions). The only exception was the gene encoding lysozyme where the control peptide was equally as effective as 6F (Fig. 10F). The control peptide that we used was selected because in a different model it was shown to be biologically inactive in preventing sphingomyelinase-induced LDL aggregation (17). This control peptide has the same 18-amino-acid residues as in the 4F peptide, but the sequence of the residues is such that α -helix formation is not promoted. In previous studies, this control peptide inhibited LDL oxidation by artery wall cells much less efficiently than the 4F sequence; however, we did not directly test the ability of this peptide to bind oxidized phospholipids (90). The oxidized phospholipids added in the ex vivo studies (Figs. 9–11) are a mixture of oxidized phospholipids that are generated by the oxidation of 1-palmitoyl-2-arachidonoyl-*sn*-glycero-3-phosphocholine. One possibility is that the decreased gene expression for lysozyme resulted from a specific oxidized phospholipid in the mixture that bound to this “control” peptide with similar affinity to 6F. Conversely, one would conclude that the oxidized phospholipids in the mixture that altered the expression of the other genes did not bind to the “control” peptide with the same affinity as they bound to the 6F peptide. Future research will be required to determine if this is the explanation for the lysozyme exception.

Mu *et al.* (93) recently reported that, in humanized mouse models of HIV that were maintained on a chow diet and treated with antiretroviral therapy to suppress plasma HIV to below detectable levels, there was evidence of gut barrier dysfunction and increased levels of LPS in plasma, which were ameliorated by

adding Tg6F (but not the EV control) to the mouse chow. Mu *et al.* (93) did not investigate intestinal mucus, they did not measure oxidized phospholipids or ROS, but they did find increased levels of oxidized lipoproteins in gut tissue in these chow-fed mice that was reduced by the addition of Tg6F. Based on the data presented here, we think that the addition of Tg6F in the studies of Mu *et al.* (93) may well have prevented an increase in oxidized phospholipids, ROS, and LPS in jejunum mucus that was responsible for their observed increase in gut permeability and increased plasma LPS levels (93).

In the studies reported in this article, addition of Tg6F to WD (but not the EV control) maintained plasma levels of SAA and IL-6 at or below those found in chow-fed mice (Fig. 8H and I, respectively, and supplemental Fig. S13A and B, respectively). However, adding Tg6F to WD only partially ameliorated the increase in plasma total cholesterol levels (supplemental Table S7). Therefore, we hypothesize that the levels of LPS largely determined the plasma levels of SAA and IL-6 in these mice. In the absence of control mice with similar plasma cholesterol levels to those in the WD + Tg6F group, we cannot definitively determine the contribution of the reduced plasma cholesterol levels in the mice receiving Tg6F to the reduced plasma levels of SAA and IL-6, but the work of Li *et al.* (35) provides support for our hypothesis.

Li *et al.* (35) found that feeding WD to *ApoE*^{-/-} mice significantly reduced the abundance of *A. muciniphila* in feces, while increasing aortic atherosclerosis. To determine if the decreased levels of *A. muciniphila* in the microbiota of the intestine played a role in the WD-mediated increase in atherosclerosis in these mice, Li *et al.* administered *A. muciniphila* by daily stomach gavage while the mice were fed WD. This resulted in a significant reduction in aortic atherosclerosis without affecting hypercholesterolemia. Oral administration of *A. muciniphila* reduced serum endotoxin levels, prevented WD-induced decreases in occludin levels in intestinal villi, increased ZO-1 levels (a tight junction protein) in intestinal villi, and largely prevented the WD-induced increase in gut permeability. To determine the role of LPS, they continued daily oral administration of *A. muciniphila* but infused LPS into the mice during the last 4 weeks of the 8 weeks during which WD was fed. This protocol achieved LPS levels similar to those seen on WD without *A. muciniphila* supplementation. Despite continuing oral administration of *A. muciniphila* during the LPS infusion, markers of systemic inflammation and the degree of aortic atherosclerosis were similar to that on WD without *A. muciniphila* supplementation. Li *et al.* (35) concluded that the beneficial effects of *A. muciniphila* were mainly due to its ability to ameliorate the WD-mediated increase in LPS levels.

Adding Tg6F to WD resulted in plasma triglyceride and plasma apoA-I levels similar to those in mice fed

chow (supplemental Table S7). However, although the WD-mediated changes in plasma total cholesterol and HDL-cholesterol levels were significantly ameliorated by adding Tg6F to WD, these levels were substantially higher and lower, respectively, compared with chow-fed mice (supplemental Table S7). Lipid absorption was not affected by adding Tg6F to WD compared with adding the EV control to WD (supplemental Figs. S4–S6). In previous studies we reported that class A amphipathic helical peptides such as 6F promoted transintestinal cholesterol efflux and promoted the removal of other lipids from intestinal tissue (9, 13), and we also reported that Tg6F increased fecal neutral sterol excretion (6). The studies reported here showed that gene expression for apoA-I in enterocytes (Fig. 4A) was higher than in chow-fed mice when Tg6F was added to WD and the content of apoA-I protein in jejunum mucus (Fig. 5E) was preserved at levels seen in chow-fed mice when Tg6F was added to WD. The maintenance of apoA-I levels after adding Tg6F to WD may explain the lower plasma total cholesterol levels and the higher HDL-cholesterol levels in mice fed WD + Tg6F compared with mice fed WD or WD + EV.

The studies reported here focused on the microbiome in jejunum mucus. The data in supplemental Fig. S2 confirm that the microbiome in jejunum mucus was distinctly different from that in the lumen of the jejunum across all four diet groups. Recent studies demonstrated that the microbiome and bile acids in the small intestine of mice can be strongly influenced by self-inoculation with fecal flora by coprophagy (94). Preventing coprophagy in mice by the use of tail cups changed the composition in the small intestine to be more similar to humans (reduced total microbial load, low abundance of anaerobic microbiota, and bile acids predominantly in the conjugated form) (94). We did not use tail cups in the experiments reported here. The comparisons between mice on the four diets used in our studies remain valid, but in extrapolating our data to humans, these differences between mice and humans must be considered.

All of the studies reported here utilized *Ldlr*^{-/-} mice. We previously reported that the response to the four diets in wild-type C57BL/6 mice was similar to that in *Ldlr*^{-/-} mice on a C57BL/6 background (5). However, the time required to see the changes after feeding the diets was considerably less in the *Ldlr*^{-/-} mice and the magnitude of the changes was considerably less in the wild-type mice (5). Thus, *Ldlr*^{-/-} mice allowed us to reduce the time for feeding the diets to only 2 weeks, which provides a substantial experimental advantage and was the reason for using these mice in the present studies.

Jejunum mucus from *Ldlr*^{-/-} mice fed WD or WD + EV had increased levels of oxidized phospholipids compared with chow-fed mice or mice receiving WD + Tg6F (Fig. 8A and supplemental Fig. S8B). The levels of

oxidized phospholipids in jejunum mucus were not different in mice fed chow compared with mice fed WD + Tg6F. In contrast to the findings in jejunum mucus, before feeding the diets to the mice, the highest level of oxidized phospholipids was in the chow diet and the 2nd highest level was in WD + Tg6F (supplemental Fig. S8A). The lowest levels of oxidized phospholipids in the diets prior to feeding the diets to the mice were in WD and WD + EV, which was opposite to the findings in jejunum mucus. By lipidomics, we found that in jejunum mucus the content of non-oxidized phosphatidylcholine, nonoxidized phosphatidylethanolamine, and nonoxidized phosphatidyl inositol significantly increased on WD compared with chow, but the levels were not different for mice receiving WD or WD + EV or WD + Tg6F (supplemental Fig. S9). The jejunum mucus content of nonoxidized phosphatidylserine was not different on any of the four diets (supplemental Fig. S9). Given these data, where do the increased oxidized phospholipids in jejunum mucus originate? There are at least three possibilities.

1) Exposing phospholipids to molecular oxygen is a standard method for preparing biologically active oxidized phospholipids (95). The molecular oxygen content of the lumen of the intestine is highest near the enterocytes and the lowest levels are in the center of the lumen (96). The molecular oxygen content of the lumen of the proximal small intestine of mice (pO₂ 60 mmHg) is high compared with that in the stomach (pO₂ 25 mmHg) and ileum (pO₂ 5 mmHg); that of the

cecum is even lower (pO₂ 1 mmHg) (30). Dietary phospholipids are absorbed in the proximal small intestine where the pO₂ in the mucus would favor phospholipid oxidation compared with the stomach, ileum, or cecum.

- 2) We previously reported finding products of mouse lipoxygenase pathways in the lumen of the proximal small intestine of *Ldlr*^{-/-} mice fed WD (97). Lipoxygenase pathway products are known to enhance the generation of biologically active oxidized phospholipids (95, 98).
- 3) The normal life cycle of enterocytes also likely leads to the formation of oxidized phospholipids. Enterocytes constantly migrate along the villus walls until they are shed from the villus tips 3–5 days after they emerged from the crypts (99). Dietary fat can induce apoptosis of enterocytes and increase gut permeability (100). Apoptotic cells express oxidized phospholipids that are recognized by the E06 antibody (101). Vesicles and blebs from apoptotic cells contain biologically active oxidized phospholipids (102).

Thus, there are multiple potential sources that could account for the increased levels of oxidized phospholipids and ROS that we found in the jejunum mucus of *Ldlr*^{-/-} mice fed WD.

We hypothesize that by preventing the WD-mediated increase in oxidized phospholipids and ROS in jejunum mucus, Tg6F preserves levels of *A. muciniphila* in mucus sufficient to prevent the increase in gut-derived LPS in mesenteric lymph and plasma that drives systemic inflammation on WD.

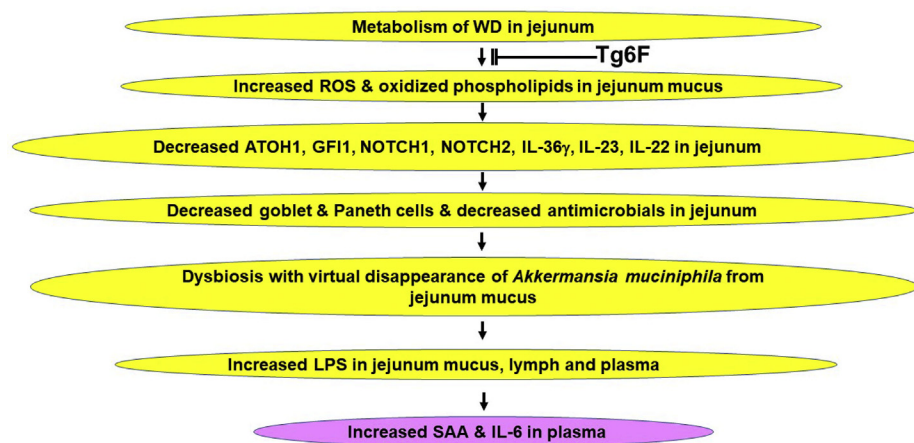


Fig. 12. A schematic representation of how the metabolism of a Western diet (WD) in the jejunum of *Ldlr*^{-/-} mice could lead to systemic inflammation, and how apoA-I mimetics such as in a concentrate of transgenic tomatoes expressing the 6F peptide (Tg6F) could prevent this sequence of events. The metabolism of WD in the jejunum leads to increased levels of reactive oxygen species (ROS) and oxidized phospholipids in jejunum mucus. This leads to decreased levels of proteins required for the formation of functional goblet and Paneth cells in jejunum (ATOH1 and GFII) and decreased levels of signaling molecules (Notch1 and Notch2) and interleukins (IL-36 γ , IL-23, and IL-22) that are necessary for maintaining antimicrobial activity in jejunum. As a result, there are decreased numbers of goblet and Paneth cells and decreased antimicrobials in jejunum. Consequently, dysbiosis results including the virtual disappearance of a species (*Akkermansia muciniphila*) that is important for maintaining healthy mucus and regulating the levels of bacterial lipopolysaccharide (LPS) in mucus. This leads to increased levels of LPS in jejunum mucus, lymph, and plasma, which in turn leads to systemic inflammation (increased levels of serum amyloid A [SAA] and IL-6 in plasma). Tg6F protects against the increase in ROS and oxidized phospholipids, thus ameliorating this sequence of events.


The ability of the oxidized phospholipids that are generated on feeding WD to profoundly decrease *A. muciniphila* in jejunum mucus may be direct or indirect. WD resulted in dysbiosis in jejunum mucus. The data in Figures 9–11 show that adding oxidized phospholipids ex vivo to jejunum from mice on a chow diet reproduced the changes in vivo in jejunum from mice that were fed WD. These changes very likely explain the dysbiosis in jejunum mucus that occurred when the mice were fed WD (Fig. 2). The ability of WD-generated oxidized phospholipids to induce dysbiosis could explain the decrease in *A. muciniphila* even without a direct effect of oxidized phospholipids on *A. muciniphila*. Future studies to determine the effect of oxidized phospholipids on *A. muciniphila* growth and viability in vitro would help to determine if oxidized phospholipids have a direct effect on *A. muciniphila*.

The importance of LPS entering through the small intestine was recently emphasized by Han *et al.* (103). These authors demonstrated that HDL₃ generated in the small intestine is directly transported into the portal circulation. They showed that HDL₃ bound LBP and LPS in such a way as to prevent the LPS from binding to TLR4 and activating liver macrophages to cause hepatic inflammation. We did not study this pathway in our experiments. However, our data apply to their observations in that the burden of LPS in small intestine mucus would affect both the chylomicron to lymphatic and the HDL to portal vein pathways. The fact that two pathways evolved for managing small intestine derived LPS speaks to the potential negative impact that this source of LPS must have. The ability of Tg6F to prevent the WD-mediated increase in oxidized phospholipids in the small intestine that leads to an increased burden of LPS in small intestine mucus, lymph, and blood suggests that preventing the increase in oxidized phospholipids in small intestine mucus may be another potential therapeutic means to protect the liver against gut-derived LPS.

In summary, the metabolism of WD in the jejunum of *Ldlb^{-/-}* mice led to increased levels of ROS and oxidized phospholipids in jejunum mucus. Feeding WD to *Ldlb^{-/-}* mice resulted in decreased levels of proteins in jejunum required for the formation of functional goblet and Paneth cells, and the number of goblet and Paneth cells in jejunum decreased. Feeding WD to *Ldlb^{-/-}* mice also resulted in decreased levels of proteins that are critical for signaling pathways, which are required for maintaining antimicrobial activity in jejunum. Dysbiosis accompanied the loss of antimicrobial activity in jejunum, and *A. muciniphila* virtually disappeared from jejunum mucus, but overall numbers of bacteria in jejunum mucus increased, and LPS increased in jejunum mucus, as well as in mesenteric lymph and plasma. Plasma markers of systemic inflammation increased. Remarkably, adding Tg6F to WD ameliorated these changes. Addition of oxidized phospholipids ex vivo to jejunum from mice fed a chow

diet reproduced the changes in jejunum gene expression that were seen in vivo when the mice were fed WD, and adding 6F peptide prevented the changes. Figure 12 presents a schematic representation of the data. The data in this article identify an important role for oxidized phospholipids in the mucus of the jejunum in causing dysbiosis and systemic inflammation and provide strong evidence that the mechanism of action of oral apoA-I mimetic peptides in mice fed WD is to protect against the increased levels of oxidized phospholipids that are formed on this diet.

Data availability

All data are contained within the article and in supplemental data. 

Supplemental data

This article contains [supplemental data](#).

Author contributions

S. T. R. and A. M. F. conceptualization; P. M., A. C., V. G., N. D., V. L., J. P. J., and B. L. C. methodology; P. M., A. C., and V. G. validation; S. T. R. and A. M. F. formal analysis; P. M., V. G., N. D., V. L., J. P. J., B. L. C., and T. V. investigation; A. M. F. writing—original draft; P. M., A. C., J. P. J., J. J. M., M. N., and S. T. R. writing—review and editing; V. L., J. P. J., T. V., and J. J. M. visualization; S. T. R. and A. M. F. supervision; S. T. R. and A. M. F. project administration; A. M. F. funding acquisition.

Author ORCIDs

Venu Lagishetty  <https://orcid.org/0000-0001-6500-8255>
Jonathan P. Jacobs  <https://orcid.org/0000-0003-4698-0254>
Thomas Vallim  <https://orcid.org/0000-0001-7642-5046>
Julia J. Mack  <https://orcid.org/0000-0002-9239-8436>

Funding and additional information

This work was supported in part by US Public Health Service Research Grant IR01 HL148286 (A. M. F.) and the Laubisch, Castera, and M. K. Grey Funds at the University of California at Los Angeles. J. P. J. and V. L. were supported by VA CDA2 IK2CX001717 and NIH/NIDDK P30 DK041301. The content is solely the responsibility of the authors and does not necessarily represent the official views of the National Institutes of Health.

Conflict of interest

A. M. F., M. N., and S. T. R. are principals in Bruin Pharma and A. M. F. is an officer in Bruin Pharma. All other authors declare that they have no conflicts of interest with the contents of this article.

Abbreviations

4F, the peptide D-W-F-K-A-F-Y-D-K-V-A-E-K-F-K-E-A-F with end blocking groups; 6F, the peptide D-W-L-K-A-F-Y-D-K-F-F-E-K-F-K-E-F-F without end blocking groups; apoA-I, apolipoprotein A-I; ATOH1, atonal homolog 1; EV, transgenic tomatoes expressing the control marker protein, β -glucuronidase; GFIL, growth factor independent protein 1;

HDL, high density lipoprotein; *Ldlr*^{-/-}, low density lipoprotein receptor null; LPS, lipopolysaccharide; LPB, LPS-binding protein; Ox-PAPC, oxidized 1-palmitoyl-2-arachidonoyl-*sn*-glycero-3-phosphocholine; REG3A, regenerating islet-derived family members 3A; ROS, reactive oxygen species; SAA, serum amyloid A; Tg6F, transgenic tomatoes expressing the 6F peptide; WD, Western diet.

Manuscript received April 7, 2021, and in revised form October 26, 2021. Published, JLR Papers in Press, November 20, 2021, <https://doi.org/10.1016/j.jlrl.2021.100153>

REFERENCES

- Chattopadhyay, A., Navab, M., Hough, G., Gao, F., Meriwether, D., Grijalva, V., Springstead, J. R., Palgunachari, M. N., Namiri-Kalantari, R., Su, F., Van Lenten, B. J., Wagner, A. C., Anantharamaiah, G. M., Farias-Eisner, R., Reddy, S. T., *et al.* (2013) A novel approach to oral apoA-I mimetic therapy. *J. Lipid Res.* **54**, 995–1010
- Navab, M., Hough, G., Buga, G. M., Su, F., Wagner, A. C., Meriwether, D., Chattopadhyay, A., Gao, F., Farias-Eisner, R., Smyth, S. S., Reddy, S. T., and Fogelman, A. M. (2013) Transgenic 6F tomatoes act on the small intestine to prevent systemic inflammation and dyslipidemia caused by Western Diet and intestinally derived lysophosphatidic acid. *J. Lipid Res.* **54**, 3403–3418
- Navab, M., Chattopadhyay, A., Hough, G., Meriwether, D., Fogelman, S. I., Wagner, A. C., Grijalva, V., Su, F., Anantharamaiah, G. M., Hwang, L. H., Faull, K. F., Reddy, S. T., and Fogelman, A. M. (2015) Source and role of intestinally derived lysophosphatidic acid in dyslipidemia and atherosclerosis. *J. Lipid Res.* **56**, 871–887
- Chattopadhyay, A., Grijalva, V., Hough, G., Su, F., Mukherjee, P., Farias-Eisner, R., Anantharamaiah, G. M., Faull, K. F., Hwang, L. H., Navab, M., Fogelman, A. M., and Reddy, S. T. (2015) Efficacy of tomato concentrates in mouse models of dyslipidemia and cancer. *Pharmacol. Res. Perspect.* **3**, e00154
- Chattopadhyay, A., Navab, M., Hough, G., Grijalva, V., Mukherjee, P., Fogelman, H. R., Hwang, L. H., Faull, K. F., Lusic, A. J., Reddy, S. T., and Fogelman, A. M. (2016) Tg6F ameliorates the increase in oxidized phospholipids in the jejunum of mice fed unsaturated LysoPC or WD. *J. Lipid Res.* **57**, 832–847
- Mukherjee, P., Hough, G., Chattopadhyay, A., Navab, M., Fogelman, H. R., Meriwether, D., Williams, K., Bensinger, S., Moller, T., Faull, K. F., Lusic, A. J., Iruela-Arispe, M. L., Bostrom, K. I., Tontonoz, P., Reddy, S. T., *et al.* (2017) Transgenic tomatoes expressing the 6F peptide and ezetimibe prevent diet-induced increases of IFN- β and cholesterol 25-hydroxylase in jejunum. *J. Lipid Res.* **58**, 1636–1647
- Chattopadhyay, A., Yang, X., Mukherjee, P., Sulaiman, D., Fogelman, H. R., Grijalva, V., Dubinett, S., Wasler, T. C., Paul, M. K., Salehi-Rad, R., Mack, J. J., Iruela-Arispe, M. L., Navab, M., Fogelman, A. M., and Reddy, S. T. (2018) Treating the intestine with oral apoA-I mimetic Tg6F reduces tumor burden in mouse models of metastatic lung cancer. *Sci. Rep.* **8**, 9032
- Mukherjee, P., Hough, G., Chattopadhyay, A., Grijalva, V., O'Connor, E. I., Meriwether, D., Wagner, A., Ntambi, J. M., Navab, M., Reddy, S. T., and Fogelman, A. M. (2018) Role of enterocyte stearoyl-Co-A desaturase-1 in LDLR-null mice. *J. Lipid Res.* **59**, 1818–1840
- Meriwether, D., Sulaiman, D., Volpe, C., Dorfman, A., Grijalva, V., Dorreh, N., Solorzano-Vargas, R. S., Wang, J., O'Connor, E., Papesh, J., Larauche, M., Trost, H., Palgunachari, M. N., Anantharamaiah, G. M., Herschman, H. R., *et al.* (2019) Apolipoprotein A-I mimetics mitigate intestinal inflammation in COX2-dependent inflammatory bowel disease model. *J. Clin. Invest.* **130**, 3670–3685
- Zhao, Y., Black, A. S., Bonnet, D. J., Mayanoff, B. E., Curtiss, L. K., Leman, L. J., and Ghadiri, M. R. (2014) In vivo efficacy of HDL-like nanolipid particles containing multivalent peptide mimetics of apolipoprotein A-I. *J. Lipid Res.* **55**, 2053–2063
- Wool, G. D., Reardon, C. A., and Getz, G. S. (2014) Mimetic peptides of human apoA-I helix 10 get together to lower lipids and ameliorate atherosclerosis: is the action in the gut? *J. Lipid Res.* **55**, 1983–1985
- Navab, M., Reddy, S. T., Anantharamaiah, G. M., Imaizumi, S., Hough, G., Hama, S., and Fogelman, A. M. (2011) Intestine may be a major site of action for the apoA-I mimetic peptide 4F whether administered subcutaneously or orally. *J. Lipid Res.* **52**, 1200–1210
- Meriwether, D., Sulaiman, D., Wagner, A., Grijalva, V., Kaji, I., Williams, K. J., Yu, L., Fogelman, S., Volpe, C., Bensinger, S. J., Anantharamaiah, G. M., Schechter, I., Fogelman, A. M., and Reddy, S. T. (2016) Transintestinal transport of the anti-inflammatory drug 4F and the modulation of transintestinal efflux. *J. Lipid Res.* **57**, 1175–1193
- Johansson, M. E. V., Phillipson, M., Petersson, J., Velich, A., Holm, L., and Hansson, G. C. (2008) The inner of the two Muc2 mucin-dependent mucus layers in colon is devoid of bacteria. *Proc. Natl. Acad. Sci. U. S. A.* **105**, 15064–15069
- Johansson, M. E. V., Holmen Larsson, J. M., and Hansson, G. C. (2011) The two mucus layers of colon are organized by the Muc2 mucin, whereas the outer layer is a legislator of host-microbial interactions. *Proc. Natl. Acad. Sci. U. S. A.* **108**, 4659–4665
- Ermund, A., Schutte, A., Johansson, M. E. V., Gustafsson, J. K., and Hansson, G. C. (2013) Studies of mucus in mouse stomach, small intestine and colon. I. Gastrointestinal mucus layers have different properties depending on location as well as over the Peyer's patches. *Am. J. Physiol. Gastrointest. Liver Physiol.* **305**, G341–G347
- Nguyen, S. D., Javanainen, M., Rissanen, S., Zhao, H., Huusko, J., Kivela, A. M., Yla-Herttuala, S., Navab, M., Fogelman, A. M., Vattulainen, L., Kovanen, P. T., and Oorni, K. (2015) Apolipoprotein A-I mimetic peptide 4F blocks sphingomyelinase-induced LDL aggregation. *J. Lipid Res.* **56**, 1206–1221
- Sevick-Muraca, E. M., Kwon, S., and Rasmussen, J. C. (2014) Emerging lymphatic imaging technologies for mouse and man. *J. Clin. Invest.* **124**, 905–914
- Nagahashi, M., Yamada, A., Aoyagi, T., Allegood, J., Wakai, T., Spiegel, S., and Takabe, K. (2016) Sphingosine-1-phosphate in the lymphatic fluid determined by novel methods. *Heliyon*. **2**, e00219
- An, Y. A., and Scherer, P. E. (2020) Mouse adipose tissue protein extraction. *Bio. Protoc.* **10**, e3631
- Hsieh, W. Y., Williams, K. J., Su, B., and Bensinger, S. J. (2020) Profiling of mouse macrophage lipidome using direct infusion shotgun mass spectrometry. *STAR Protoc.* **2**, 100235
- Jandacek, R. J., Heubi, J. E., and Tso, P. (2004) A novel, noninvasive method for the measurement of intestinal fat absorption. *Gastroenterology*. **127**, 139–144
- Jacobs, J. P., Lin, L., Goudarzi, M., Ruegger, P., McGovern, D. P. B., Fornace, A. J., Borneman, J., Xia, L., and Braun, J. (2017) Microbial, metabolomic, immunologic dynamics in a relapsing genetic mouse model of colitis induced by T-synthase deficiency. *Gut Microbes*. **8**, 1–16
- Callahan, B. J., McMurdie, P. J., Rosen, M. J., Han, A. W., Johnson, A. J. A., and Holmes, S. P. (2016) DADA2: high-resolution sample inference from Illumina amplicon data. *Nat. Methods*. **13**, 581–583
- Nadkarni, M. A., Martin, F. E., Jacques, N. A., and Hunter, N. (2002) Determination of bacterial load by real-time PCR using a broad-range (universal) probe and primers set. *Microbiology*. **148**, 257–266
- Love, M. I., Huber, W., and Anders, S. (2014) Moderated estimation of fold change and dispersion for RNA-seq data with DESeq2. *Genome Biol.* **15**, 550
- Storey, J. D., and Tibshirani, R. (2003) Statistical significance for genomewide studies. *Proc. Natl. Acad. Sci. U. S. A.* **100**, 9440–9445
- Goodrich, J. K., Di Rienzi, S. C., Poole, A. C., Koren, O., Walters, W. A., Caporaso, J. G., Knight, R., and Ley, R. E. (2014) Conducting a microbiome study. *Cell*. **158**, 250–262
- Kim, B.-R., Shin, J., Guevarra, R. B., Lee, J. H., Kim, D. W., Seol, K.-H., Lee, J.-H., Kim, H. B., and Isaacson, R. E. (2017) Deciphering diversity indices for a better understanding of microbial communities. *J. Microbiol. Biotechnol.* **27**, 2089–2093
- Friedman, E. S., Bittinger, K., Espipova, T. V., Hou, L., Chau, L., Jiang, J., Mesaros, C., Lund, P. J., Liang, X., FitzGerald, G. A., Goulian, M., Lee, D., Garcia, B. A., Blair, I. A., Vinogradov, S. A.,

- et al.* (2018) Microbes vs. chemistry in the origin of the anaerobic gut lumen. *Proc. Natl. Acad. Sci. U. S. A.* **115**, 4170–4175
31. Paone, P., and Cani, P. D. (2020) Mucus barrier, mucins and gut microbiota: the expected slimy partners? *Gut* **69**, 2232–2243
 32. Hiippala, K., Jouhten, H., Ronkainen, A., Hartikainen, A., Kainulainen, V., Jalanka, J., and Satokari, R. (2018) The potential of gut commensals in reinforcing intestinal barrier function and alleviating inflammation. *Nutrients* **10**, 988
 33. Everard, A., Belzer, C., Geurts, L., Ouwerkerk, J. P., Druart, C., Bindels, L. B., Guiot, Y., Derrien, M., Muccioli, G. G., Dezenne, N. M., de Vos, W. M., and Cani, P. D. (2013) Cross-talk between *Akkermansia muciniphila* and intestinal epithelium controls diet-induced obesity. *Proc. Natl. Acad. Sci. U. S. A.* **110**, 9066–9071
 34. Plovier, H., Everard, A., Druart, C., Depommier, C., Van Hul, M., Geurts, L., Chilloux, J., Ottman, N., Duparc, T., Lichtenstein, L., Myridakis, A., Delzenne, N. M., Klievink, J., Bhattacharjee, A., van der Ark, K. C. H., *et al.* (2017) A purified membrane protein from *Akkermansia muciniphila* or the pasteurized bacterium improves metabolism in obese and diabetic mice. *Nat. Med.* **23**, 107–113
 35. Li, J., Lin, S., Vanhoutte, P. M., Woo, C. W., and Xu, A. (2016) *Akkermansia muciniphila* protects against atherosclerosis by preventing metabolic endotoxemia-induced inflammation in *ApoE*^{-/-} mice. *Circulation* **133**, 2434–2446
 36. Greer, R. L., Dong, X., Moraes, A. C. F., Zielke, R. A., Fernandes, G. R., Peremyslova, E., Vasquez-Perez, S., Schoenborn, A. A., Gomes, E. P., Pereira, A. C., Ferreira, S. R. G., Yao, M., Fuss, I. J., Strober, W., Sikora, A. E., *et al.* (2016) *Akkermansia muciniphila* mediates negative effects of IFN γ on glucose metabolism. *Nat. Commun.* **7**, 13329
 37. Depommier, C., Van Hul, M., Everard, A., Delzenne, N. M., De Vos, W. M., and Cani, P. D. (2020) Pasteurized *Akkermansia muciniphila* increases whole-body energy expenditure and fecal energy excretion in diet-induced obese mice. *Gut Microbes* **11**, 1231–1245
 38. Reunanen, J., Kainulainen, V., Huuskonen, L., Ottman, N., Belzer, C., Huhtinen, H., de Vos, W. M., and Satokari, R. (2015) *Akkermansia muciniphila* adheres to enterocytes and strengthens the integrity of the epithelial cell layer. *Appl. Environ. Microbiol.* **81**, 3655–3662
 39. Depommier, C., Everard, A., Druart, C., Plovier, H., Van Hul, M., Vieira-Silva, S., Falony, G., Raes, J., Maiter, D., Delzenne, N. M., de Barse, M., Loumave, A., Hermans, M. P., Thissen, J.-P., de Vos, W. M., *et al.* (2019) Supplementation with *Akkermansia muciniphila* in overweight and obese human volunteers: a proof-of-concept exploratory study. *Nat. Med.* **25**, 1096–1103
 40. Druart, C., Plovier, H., Van Hul, M., Brient, A., Phipps, K. R., de Vos, W. M., and Cani, P. D. (2021) Toxicological safety evaluation of pasteurized *Akkermansia muciniphila*. *J. Appl. Toxicol.* **41**, 276–290
 41. Ottman, N., Reunanen, J., Meijerink, M., Pietila, T. E., Kainulainen, V., Klievink, J., Huuskonen, L., Aalvink, S., Skurnik, M., Boeren, S., Satokari, R., Mercenier, A., Palva, A., Smidt, H., de Vos, W. M., *et al.* (2017) Pili-like proteins of *Akkermansia muciniphila* modulate host immune responses and gut barrier function. *PLoS One* **12**, e0173004
 42. Dao, M. C., Everard, A., Aron-Wisnewsky, J., Sokolovska, N., Prifti, E., Verger, E. O., Kayser, B. D., Levenez, F., Chilloux, J., Hoyles, L., MICRO-Obes Consortium, Dumas, M.-E., Rizkalla, S. W., Dore, J., Cani, P. D., and Clement, K. (2016) *Akkermansia muciniphila* and improved metabolic health during a dietary intervention in obesity: relationship with gut microbiome richness and ecology. *Gut* **65**, 426–436
 43. Geerlings, S. Y., Kostopoulos, I., de Vos, W. M., and Belzer, C. (2018) *Akkermansia muciniphila* in the human gastrointestinal tract: when, where, and how? *Microorganisms* **6**, 75
 44. Cash, H. L., Whitham, C. V., Behrendt, C. L., and Hopper, L. V. (2006) Symbiotic bacteria direct expression of an intestinal bactericidal lectin. *Science* **313**, 1126–1130
 45. Mohandas, S., and Vairappan, B. (2020) Ginkgolide-A attenuates bacterial translocation through activating PXR and improving antimicrobial peptide Reg 3A in experimental cirrhosis. *Life Sci.* **257**, 118111
 46. Cao, S., Su, X., Zeng, B., Yan, H., Huang, Y., Wang, E., Yun, H., Zhang, Y., Liu, F., Li, W., Wei, H., Che, Y., and Yang, R. (2016) The gut epithelial receptor LRRCL19 promotes the recruitment of immune cells and gut inflammation. *Cell Rep.* **14**, 695–707
 47. Wang, L., Fouts, D. E., Starkel, P., Hartmann, P., Chen, P., Llorente, C., DePew, J., Moncera, K., Ho, S. B., Brenner, D. A., Hooper, L. V., and Schnabl, B. (2016) Intestinal REG3 lectins protect against steatohepatitis by reducing mucosa-associated microbiota and preventing bacterial translocation. *Cell Host Microbe* **19**, 227–239
 48. van Ampting, M. T. J., Loonen, M. P., Schonewille, A. J., Konings, I., Vink, C., Iovanna, J., Chamailard, M., Dekker, J., van der Meer, R., Wells, J. M., and Bovee-Oudenhoven, I. M. J. (2012) Intestinally secreted C-type lectin Reg3b attenuates salmonellosis but not listeriosis in mice. *Infect. Immun.* **80**, 1115–1120
 49. Vaishnav, S., Yamamoto, M., Severson, K. M., Ruhn, K. A., Yu, X., Koren, O., Ley, R., Wakeland, E. K., and Hooper, L. V. (2011) The antibacterial lectin RegIII γ promotes the spatial segregation of microbiota and host in the intestine. *Science* **334**, 255–258
 50. Salzman, N. H., Underwood, M. A., and Bevins, C. L. (2007) Paneth cells, defensins, and the commensal microbiota: a hypothesis on intimate interplay at the intestinal mucosa. *Semin. Immunol.* **19**, 70–83
 51. Bals, R., Wang, X., Meegalla, R. L., Wattler, S., Weiner, D. J., Nehls, M. C., and Wilson, J. M. (1999) Mouse β -defensin 3 is an inducible antimicrobial peptide expressed in the epithelia of multiple organs. *Infect. Immun.* **67**, 3542–3547
 52. Rahman, A., Fahlgren, A., Sundstedt, C., Hammarstrom, S., Danielsson, A., and Hammarstrom, M. L. (2011) Chronic colitis induces expression of β -defensins in murine intestinal epithelial cells. *Clin. Exp. Immunol.* **163**, 123–130
 53. Fahlgren, A., Hammarstrom, S., Danielsson, A., and Hammarstrom, M.-L. (2004) β -defensin-3 and -4 in intestinal epithelial cells display increased mRNA expression in ulcerative colitis. *Clin. Exp. Immunol.* **137**, 379–385
 54. Peeters, T., and Vantrappen, G. (1975) The paneth cell: A source of intestinal lysozyme. *Gut* **16**, 553–558
 55. Goldberg, R. F., Austen, W. G., Zhang, X., Munene, G., Mostafa, G., Biswas, S., McCormack, M., Eberlin, K. R., Nguyen, J. T., Tatlidede, H. S., Warren, H. S., Narisawa, S., Millan, J. L., and Hodin, R. A. (2008) Intestinal alkaline phosphatase is a gut mucosal defense factor maintained by enteral nutrition. *Proc. Natl. Acad. Sci. U. S. A.* **105**, 3551–3556
 56. Narisawa, S., Huang, L., Iwasaki, A., Hasegawa, H., Alpers, D. H., and Millan, J. L. (2003) Accelerated fat absorption in intestinal alkaline phosphatase knockout mice. *Mol. Cell Biol.* **23**, 7525–7530
 57. Madsen, J., Mollenhauer, J., and Holmskov, U. (2010) Gp-340/DMBT1 in mucosal innate immunity. *Innate Immun.* **16**, 160–167
 58. Fukui, H., Sekikawa, A., Tanaka, H., Fujimori, Y., Katake, Y., Fujii, S., Ichikawa, K., Tomita, S., Imura, J., Chiba, T., and Fujimori, T. (2011) DMBT1 is a novel gene induced by IL-22 in ulcerative colitis. *Inflamm. Bowel Dis.* **17**, 1177–1188
 59. Rosenstiel, P., Sina, C., End, C., Renner, M., Lyer, S., Till, A., Hellmig, S., Nikolaus, S., Folsch, U. R., Helmke, B., Autschbach, F., Schirmacher, P., Kioschis, P., Hafner, M., Poustka, A., *et al.* (2007) Regulation of DMBT1 via NOD2 and TLR4 in intestinal epithelial cells modulates bacterial recognition and invasion. *J. Immunol.* **178**, 8203–8211
 60. Pelaseyed, T., Bergstrom, J. H., Gustafsson, J. K., Ermund, A., Birchenough, G. M. H., Schutte, A., van der Post, S., Svensson, F., Rodriguez-Pineiro, A. M., Nystrom, E. E. L., Wising, C., Johansson, M. E. V., and Hansson, G. C. (2014) The mucus and mucins of the goblet cells and enterocytes provide the first defense line of the gastrointestinal tract and interact with the immune system. *Immunol. Rev.* **260**, 8–20
 61. Guo, X.-K., Ou, J., Liang, S., Zhou, X., and Hu, X. (2018) Epithelial Hes1 maintains gut homeostasis by preventing microbial dysbiosis. *Mucosal Immunol.* **11**, 716–726
 62. Ma, J., Liao, X.-L., Lou, B., and Wu, M.-P. (2004) Role of apolipoprotein A-I in protecting against endotoxin toxicity. *Acta Biochim. Biophys. Sin.* **36**, 419–424
 63. Thaveeratitham, P., Plengpanich, W., Naen-Udorn, W., Patumraj, S., and Khovidhunkit, W. (2007) Effects of human apolipoprotein A-I on endotoxin-induced leukocyte adhesion on endothelial cells *in vivo* and on the growth of *Escherichia coli in vitro*. *J. Endotoxin Res.* **13**, 58–64
 64. Beck, W. H. J., Adams, C. P., Biglang-awa, I. M., Patel, A. B., Vincent, H., Haas-Stapleton, E. J., and Weers, P. M. M. (2013) Apolipoprotein A-I binding to anionic vesicles and

- lipopolysaccharides: role for lysine residues in antimicrobial properties. *Biochim. Biophys. Acta*. **1828**, 1503–1510
65. Rubio, S., Lacaze-Masmonteil, T., Chailley-Heu, B., Kahn, A., Bourbon, J. R., and Ducroc, R. (1995) Pulmonary surfactant A (SP-A) is expressed by epithelial cells of small and large intestine. *J. Biol. Chem.* **270**, 12162–12169
 66. Eliakim, R., Goetz, G., Rubio, S., Chailley-Heu, B., Shao, J-S., Ducroc, R., and Alpers, D. H. (1997) Isolation and characterization of surfactant-like particles in rat and human colon. *Am. J. Physiol.* **272**, G425–G434
 67. Wu, H., Kuzmenko, A., Wan, S., Schaffer, L., Weiss, A., Fisher, J. H., Kim, K. S., and McCormack, F. X. (2003) Surfactant proteins A and D inhibit the growth of gram-negative bacteria by increasing membrane permeability. *J. Clin. Invest.* **113**, 1589–1602
 68. Hansen, G. H., Rasmussen, K., Niels-Christiansen, L-L., and Danielsen, E. M. (2009) Lipopolysaccharide-binding protein: localization in secretory granules of paneth cells in mouse small intestine. *Histochem. Cell Biol.* **131**, 727–732
 69. Vreugdenhil, A. C., Snoek, A. M. P., Greve, J. W. M., and Buurman, W. A. (2000) Lipopolysaccharide-binding protein is vectorially secreted and transported by cultured intestinal epithelial cells and is present in the intestinal mucus of mice. *J. Immunol.* **165**, 4561–4566
 70. Ito, K., Nakajima, A., Fukushima, Y., Suzuki, K., Sakamoto, K., Hamazaki, Y., Ogasawara, K., Minato, N., and Hattori, M. (2017) The potential role of osteopontin in the maintenance of commensal bacteria homeostasis in the intestine. *PLoS One* **12**, e0173629
 71. Nazmi, A., Greer, M. J., Hoek, K. L., Piazuolo, M. B., Weitkamp, J-H., and Olivares-Villagomez, D. (2020) Osteopontin and iCD8 α cells promote intestinal intraepithelial lymphocyte homeostasis. *J. Immunol.* **204**, 1968–1981
 72. Mizoguchi, A. (2012) Healing of intestinal inflammation by IL-22. *Inflamm. Bowel Dis.* **18**, 1777–1784
 73. Shih, V. F-S., Cox, J., Kljavin, N. M., Dengler, H. S., Reichelt, M., Kumar, P., Rangell, L., Kolls, J. K., Diehl, L., Ouyang, W., and Ghilardi, N. (2014) Homeostatic IL-23 receptor signaling limits Th17 response through IL-22-mediated containment of commensal microbiota. *Proc. Natl. Acad. Sci. U. S. A.* **111**, 13942–13947
 74. Parks, O. B., Pociask, D. A., Hodzic, Z., Kolls, J. K., and Good, M. (2016) Interleukin-22 signaling in the regulation of intestinal health and disease. *Front. Cell Dev. Biol.* **3**, 85
 75. Ngo, V. L., Abo, H., Maxim, E., Harusato, A., Geem, D., Medina-Contreras, O., Merlin, D., Gewirtz, A. T., Nusrat, A., and Denning, T. L. (2018) A cytokine network involving IL-36 γ , IL-23, and IL-22 promotes antimicrobial defense and recovery from intestinal barrier damage. *Proc. Natl. Acad. Sci. U. S. A.* **115**, E5076–E5085
 76. Fatkhullina, A. R., Peshkova, I. O., Dzutsev, A., Aghayev, T., McCulloch, J. A., Thovarai, V., Badger, J. H., Vats, R., Sundd, P., Tang, H-Y., Kossenkov, A. V., Hazen, S. L., Trinchieri, G., Grivennikov, S. I., and Koltsova, E. K. (2018) An interleukin-23-interleukin-22 axis regulates intestinal microbial homeostasis to protect from diet-induced atherosclerosis. *Immunity*. **49**, 943–957
 77. Bohin, N., Keeley, T. M., Carulli, A. J., Walker, E. M., Carlson, E. A., Gao, J., Aifantis, I., Siebel, C. W., Rajala, M. W., Myers, M. G., Jr., Jones, J. C., Brindley, C. D., Dempsey, P. J., and Samuelson, L. C. (2020) Rapid crypt remodeling regenerates the intestinal stem cell niche after Notch inhibition. *Stem Cell Rep.* **15**, 156–170
 78. Durand, A., Donahue, B., Peignon, G., Letourneur, F., Cagnard, N., Slomianny, C., Perret, C., Shroyer, N. F., and Romagnolo, B. (2012) Functional intestinal stem cells after Paneth cell ablation induced by the loss of transcription factor Math1 (Atoh1). *Proc. Natl. Acad. Sci. U. S. A.* **109**, 8965–8970
 79. VanDussen, K. L., Carulli, A. J., Keeley, T. M., Patel, S. R., Puthoff, B. J., Magness, S. T., Tran, I. T., Maillard, I., Siebel, C., Kolterud, A., Grosse, A. S., Gumucio, D. L., Ernst, S. A., Tsai, Y-H., Dempsey, P. J., et al. (2012) Notch signaling modulates proliferation and differentiation of intestinal crypt base columnar stem cells. *Development*. **139**, 488–497
 80. Demitrack, E. S., and Samuelson, L. C. (2016) Notch regulation of gastrointestinal stem cells. *J. Physiol.* **594**, 4791–4803
 81. Shroyer, N. F., Wallis, D., Venken, K. J. T., Bellen, H. J., and Zoghbi, H. Y. (2005) *Gfi1* functions downstream of *Math1* to control intestinal secretory cell subtype allocation and differentiation. *Genes Dev.* **19**, 2412–2417
 82. Noah, T. K., Kazanjian, A., Whitsett, J., and Shroyer, N. F. (2010) SAM pointed domain ETS factor (SPDEF) regulates terminal differentiation and maturation of intestinal goblet cells. *Exp. Cell Res.* **316**, 452–465
 83. Garcia-Hernandez, V., Quiros, M., and Nusrat, A. (2017) Intestinal epithelial claudins: expression and regulation in homeostasis and inflammation. *Ann. N. Y. Acad. Sci.* **1397**, 66–79
 84. Chelakkot, C., Ghim, J., and Ryu, S. H. (2018) Mechanisms regulating intestinal barrier integrity and its pathological implications. *Exp. Mol. Med.* **50**, 103
 85. Ghoshal, S., Witta, J., Zhong, J., de Villiers, W., and Eckhardt, E. (2009) Chylomicrons promote intestinal absorption of lipopolysaccharides. *J. Lipid Res.* **50**, 90–97
 86. Grunfeld, C., and Feingold, K. R. (2009) Endotoxin in the gut and chylomicrons: translocation or transportation? *J. Lipid Res.* **50**, 1–2
 87. Lee, J-C., Lee, H-Y., Kim, T. K., Kim, M-S., Park, Y-M., Kim, J., Park, K., Kweon, M-N., Kim, S-H., Bae, J-W., Hur, K. Y., and Lee, M-S. (2017) Obesogenic diet-induced gut barrier dysfunction and pathobiont expansion aggravate experimental colitis. *PLoS One* **12**, e0187515
 88. Briot, A., Civelek, M., Seki, A., Hoi, K., Mack, J. J., Lee, S. D., Kim, J., Hong, C., Yu, J., Fishbein, G. A., Vakili, L., Fogelman, A. M., Fishbein, M. C., Luisis, A. J., Tontonoz, P., et al. (2015) Endothelial NOTCH1 is suppressed by circulating lipids and antagonizes inflammation during atherosclerosis. *J. Exp. Med.* **212**, 2147–2163
 89. Datta, G., Chaddha, M., Hama, S., Navab, M., Fogelman, A. M., Garber, D. W., Mishra, V. K., Epanand, R. M., Epanand, R. F., Lund-Katz, S., Phillips, M. C., Segrest, J. P., and Anantharamaiah, G. M. (2001) Effects of increasing hydrophobicity on the physical-chemical and biological properties of a class A amphipathic helical peptide. *J. Lipid Res.* **42**, 1096–1104
 90. Van Lenten, B. J., Wagner, A. C., Jung, C-L., Ruchala, P., Waring, A. J., Lehrer, R. I., Watson, A. D., Hama, S., Navab, M., Anantharamaiah, G. M., and Fogelman, A. M. (2008) Anti-inflammatory apoA-I mimetic peptides bind oxidized lipids with much greater affinity than human apoA-I. *J. Lipid Res.* **49**, 2302–2311
 91. Que, X., Hung, M-Y., Yeang, C., Gonen, A., Prohaska, T., Sun, X., Diehl, C., Maatta, A., Gaddis, D. E., Bowden, K., Pattison, J., MacDonald, J. G., Yla-Herttuala, S., Mellon, P. L., Hedrick, C. C., et al. (2018) Oxidized phospholipids are proinflammatory and proatherogenic in hypercholesterolaemic mice. *Nature*. **558**, 301–306
 92. Oehler, B., Kistner, K., Martin, C., Schiller, J., Mayer, R., Mohammadi, M., Saure, R-S., Filipovic, M. R., Nieto, F. R., Kloka, J., Pflucke, D., Hill, K., Schaefer, M., Malcangio, M., Reeh, P. W., et al. (2017) Inflammatory pain control by blocking oxidized phospholipid-mediated TRP channel activation. *Sci. Rep.* **7**, 5447
 93. Mu, W., Sharma, M., Heymans, R., Ritou, E., Rezek, V., Hamid, P., Kossyvakis, A., Sen Roy, S., Grijalva, V., Chattopadhyay, A., Papesch, J., Meriwether, D., Kitchen, S. G., Fogelman, A. M., Reddy, S. T., et al. (2021) ApoA-I mimetics attenuate macrophage activation in chronic treated HIV. *AIDS*. **35**, 543–553
 94. Bogatyrev, S. R., Rolando, J. C., and Ismagilov, R. F. (2020) Self-reinoculation with fecal flora changes microbiota density and composition leading to an altered bile-acid profile in the mouse small intestine. *Microbiome*. **8**, 19
 95. Navab, M., Hama, S. Y., Anantharamaiah, G. M., Hassan, K., Hough, G. P., Watson, A. D., Reddy, S. T., Sevanian, A., Fonarow, G. C., and Fogelman, A. M. (2000) Normal high density lipoprotein inhibits three steps in the formation of mildly oxidized low density lipoprotein: steps 2 and 3. *J. Lipid Res.* **41**, 1495–1508
 96. Albenberg, L., Esipova, T. V., Judge, C. P., Bittinger, K., Chen, J., Laughlin, A., Grunberg, S., Baldassano, R. N., Lewis, J. D., Li, H., Thom, S. R., Bushman, F. D., Vinogradov, S. A., and Wu, G. D. (2014) Correlation between intraluminal oxygen gradient and radial partitioning of intestinal microbiota. *Gastroenterology*. **147**, 1055–1063
 97. Navab, M., Reddy, S. T., Anantharamaiah, G. M., Hough, G., Buga, G. M., Danciger, J., and Fogelman, A. M. (2012) D-4F-mediated reduction in metabolites of arachidonic and linoleic acids in the small intestine is associated with decreased inflammation in low-density lipoprotein receptor-null mice. *J. Lipid Res.* **53**, 437–445

98. Navab, M., Hama, S. Y., Hough, G. P., Subbanagounder, G., Reddy, S. T., and Fogelman, A. M. (2001) A cell-free assay for detecting HDL that is dysfunctional in preventing the formation of or inactivating oxidized phospholipids. *J. Lipid Res.* **42**, 1308–1317
99. Moor, A. E., Harnik, Y., Ben-Moshe, S., Massasa, E. E., Rozenberg, M., Eilam, R., Halpern, K. B., and Itzkovitz, S. (2018) Spatial reconstruction of single enterocytes uncovers broad zonation along the intestinal villus axis. *Cell* **175**, 1156–1167
100. Rohr, M. W., Narasimhulu, C. A., Rudeski-Rohr, T. A., and Parthasarathy, S. (2020) Negative effects of a high-fat diet on intestinal permeability: A review. *Adv. Nutr.* **11**, 77–91
101. Chang, M-K., Bergmark, C., Laurila, A., Horkko, S., Han, K-H., Friedman, P., Dennis, E. A., and Witztum, J. L. (1999) Monoclonal antibodies against oxidized low-density lipoprotein bind to apoptotic cells and inhibit their phagocytosis by elicited macrophages: Evidence that oxidation-specific epitopes mediate macrophage recognition. *Proc. Natl. Acad. Sci. U. S. A.* **96**, 6353–6358
102. Huber, J., Vales, A., Mitulovic, G., Blumer, M., Schmid, R., Witztum, J. L., Binder, B. R., and Leitinger, N. (2002) Oxidized membrane vesicles and blebs from apoptotic cells contain biologically active oxidized phospholipids that induce monocyte-endothelial interactions. *Arterioscler. Thromb. Vasc. Biol.* **22**, 101–107
103. Han, Y-H, Onufer, E. J., Huang, L-H, Sprung, R. W., Davidson, W. S., Czepielewski, R. S., Wohltmann, M., Sorci-Thomas, M. G., and Randolph, G. J. (2021) Enterically derived high-density lipoprotein restrains liver injury through the portal vein. *Science* **373**, eabe6729